



ESA-MOST Dragon Cooperation

中国科技部-欧洲空间局“龙计划”合作

2017 DRAGON 4 SYMPOSIUM

2017年“龙计划”四期学术研讨会

Three- and Four-Dimensional Topographic Measurement and Validation

(ID: 32278)

26-30 June 2017 | Copenhagen, Denmark

2017年6月26-30日, 丹麦 哥本哈根

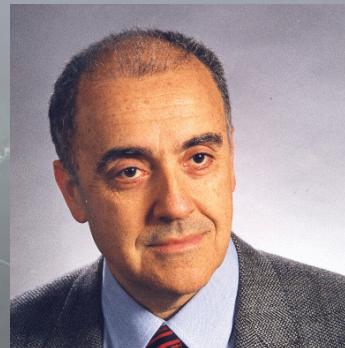
Three- and Four-Dimensional Topographic Measurement and Validation

(ID: 32278)

Prof. Deren Li



Prof. Fabio Rocca



Main objectives

- **Absolute geo-coordinate estimation** of artificial targets in optical and SAR imagery and the **validation** of their accuracy
- Digital elevation model (DEM) **generation and validation**
- **Near-real time surface motion estimation** with multi-baseline InSAR
- **Glacier motion** and 3D subsurface information retrieval
- **Polarimetric TomoSAR** analysis for forest parameter retrieval
- **Stereo-Radargrammetry analysis** for incoherent forest height change retrieval

Three research groups

1. Topographic Mapping - Validation

Prof. Timo Balz – Prof. Norbert Haala

Wuhan University – University Stuttgart

2. Multi-baseline SAR processing for 3D/4D reconstruction

Prof. Mingsheng Liao – Prof. Stefano Tebaldini

Wuhan University – POLIMI

3. Towards Near-Real Time InSAR Deformation estimation

Prof. Xiaoli Ding – Prof. Ramon Hanssen

PolyU Shenzhen Research Institute – Delft University of Technology

MULTI-BASELINE SAR PROCESSING FOR 3D/4D RECONSTRUCTION

Mingsheng LIAO¹, Lu ZHANG¹, Timo BALZ¹, Tianliang YANG², Deren LI¹

1. LIESMARS, Wuhan University, China

2. Shanghai Institute of Geological Survey, China

liao@whu.edu.cn

Main Objectives

- Continue the research on PS-InSAR based techniques and continue the work on analyzing of landslides, subsidence due to mining or underground water extraction, and seismic activity.
- Focuses on the use of polarimetric SAR tomography to investigate distributed media, such as forests and ice. This is especially valuable for the estimation of biomass in tropical and boreal forests.

Main Topics

- Multi-baseline SAR for 3D and 4D information retrieval
- Tomographic SAR analysis in urban areas
- Polarimetric TomoSAR analysis for forest parameter retrieval
- Stereo-Radargrammetry analysis for incoherent forest height change retrieval
- Glacier motion and 3D subsurface information retrieval

Research activities & Results - Part I

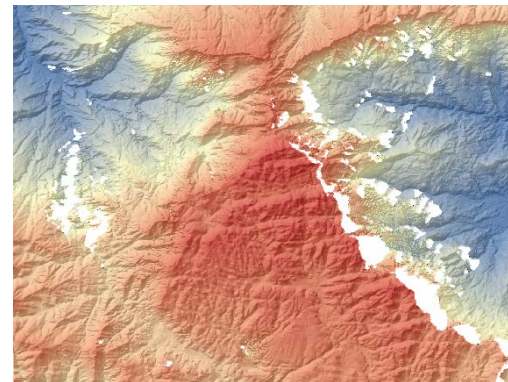
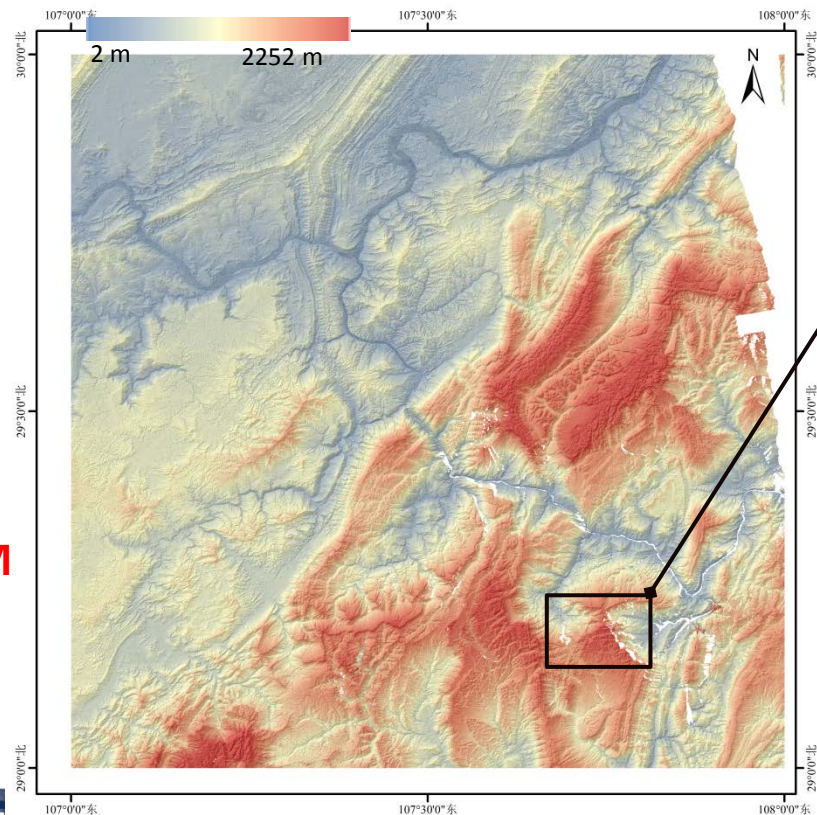
Application of InSAR Combined with StereoSAR in High-precision Topographic Mapping of Mountainous Area

Problems of InSAR technique for topographic mapping:

The height accuracy of InSAR DSM is easily affected by the interferometric phase error, which is mainly induced by the following factors:

- 1) atmospheric effect.
- 2) decorrelation factors, e.g. temporal, volume scattering decorrelation etc..
- 3) image geometric distortions caused by layover or shadow.

WorldDEM



2017 DRAGON 4 SYMPOSIUM

26-30 June 2017 | Copenhagen, Denmark

2017年“龙计划”四期学术研讨会

2017年6月26-30日, 丹麦 哥本哈根

✓ StereoSAR makes use of the **amplitude** information; InSAR takes use of the **phase** information.

✓ InSAR is more sensitive to topographic details than StereoSAR.

⇒ **Fix-up InSAR DSM data voids with StereoSAR DSM.**

✓ StereoSAR measures the **absolute slant range difference** while the interferometric phase is wrapped into $(-\pi, \pi)$.

⇒ **Calibrate the InSAR unwrapped phase with some high-precision StereoSAR height.**

StereoSAR DSM generation process

✓ StereoSAR DSM generation is composed of two steps:

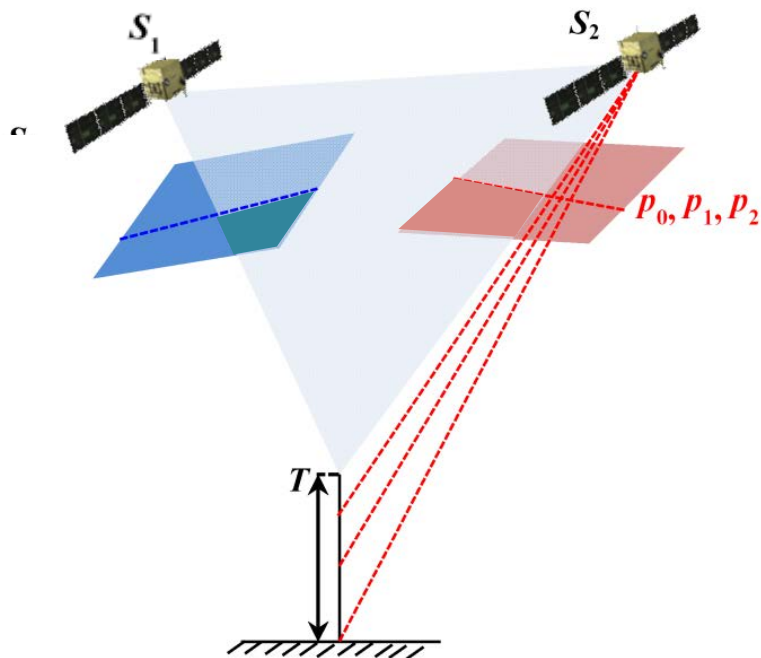
- 1) image matching to identify the homologous points;
- 2) space forward intersection to determine the ground coordinates;

✓ The bottleneck for StereoSAR is image matching especially in mountainous areas due to the severe geometric distortion.

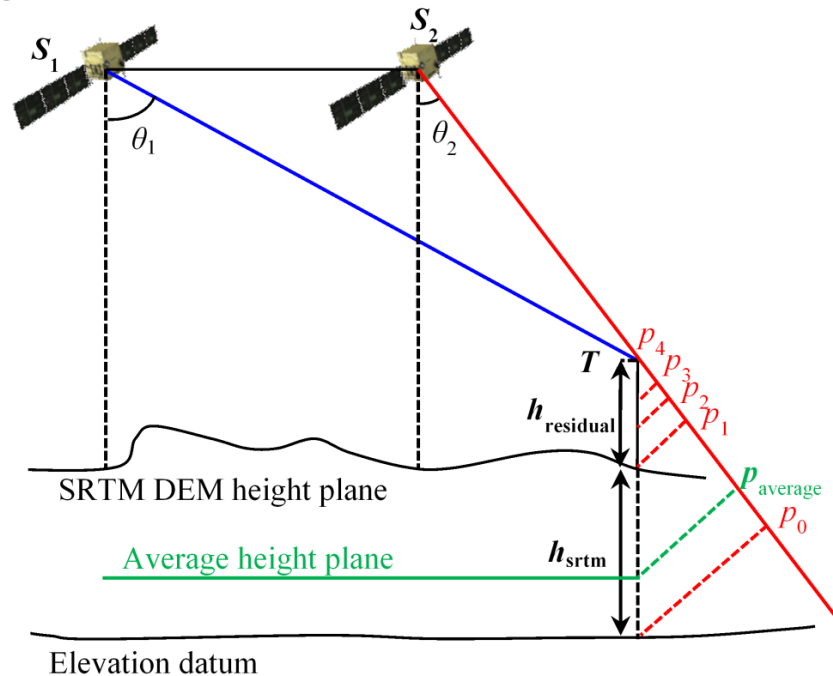


Therefore, adaptive window Least Square Matching algorithm has been proposed (AW-LSM).

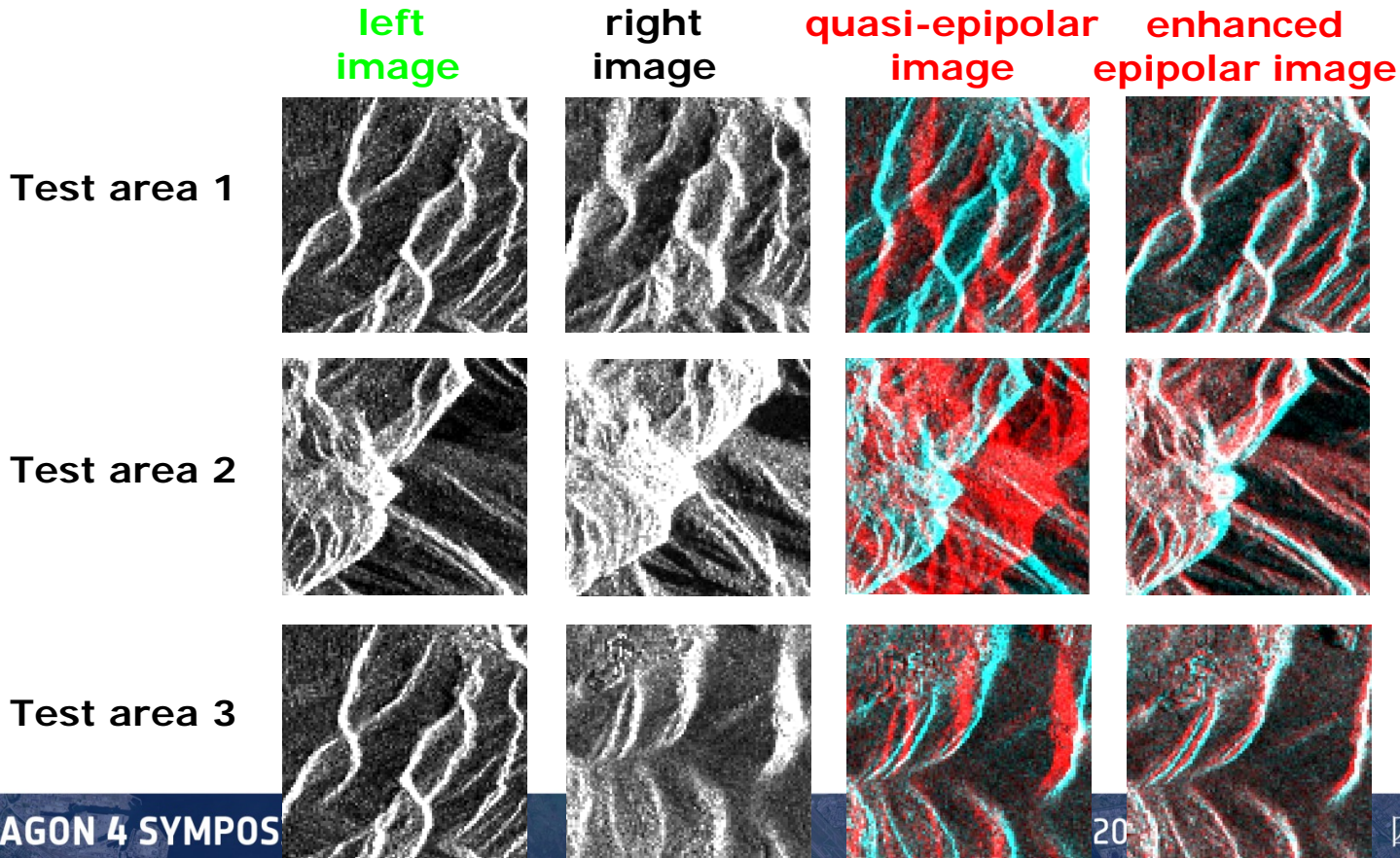
Step 1: enhanced epipolar image generation



Geometric relation of photogrammetry



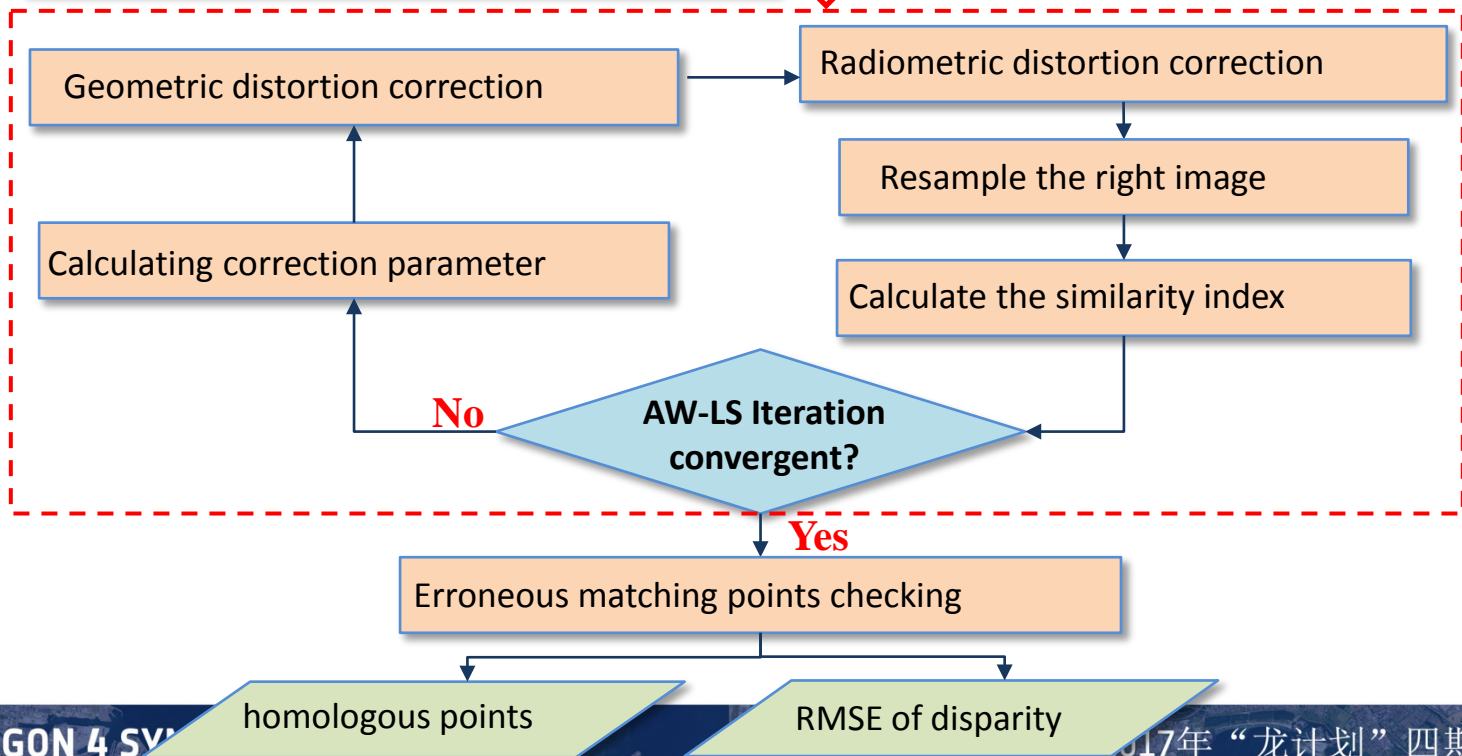
Geometric relation of radargrammetry



Start

Initialized by cross correlation process

Step 2: AW-LSM iteration

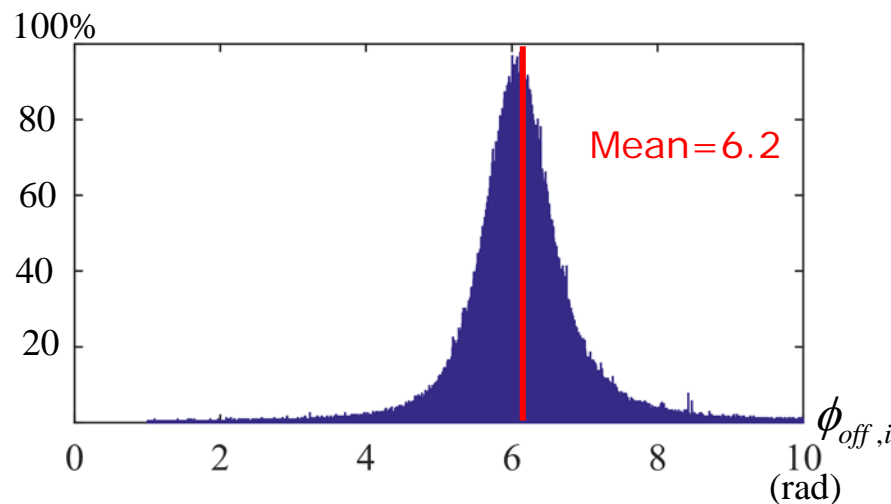


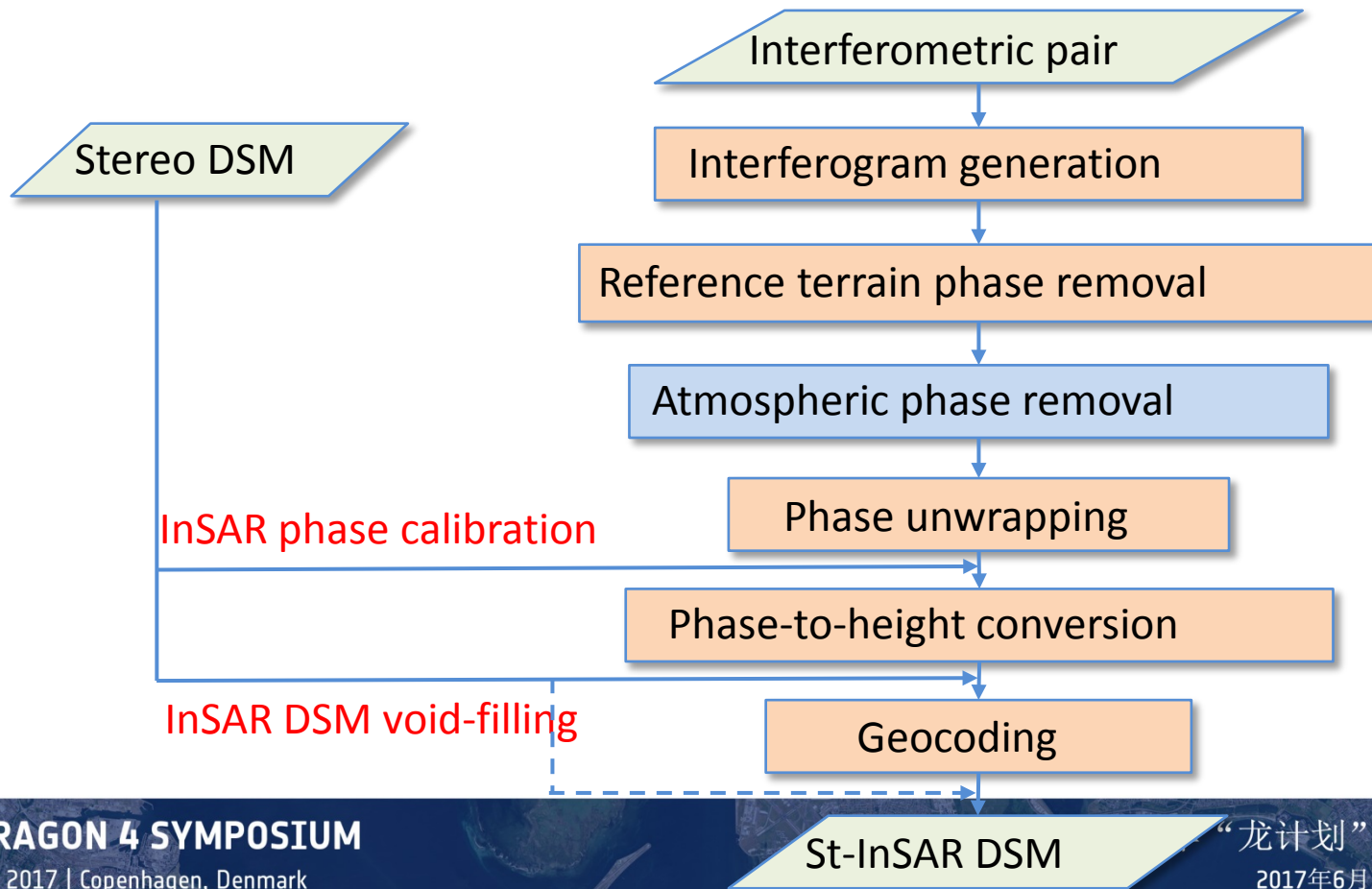
✓Collecting the sample points all over the StereoSAR DSM with **high height precision**.

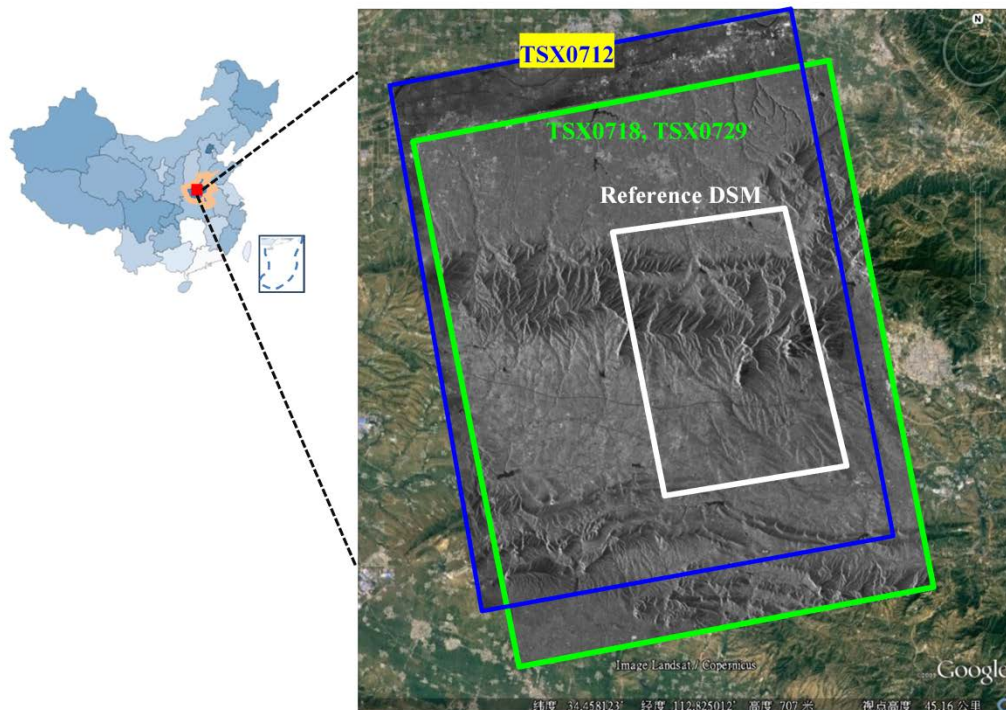
✓Calculate the $\phi_{off,i}$ for each sample points.

✓Plot the **frequency histogram** of $\phi_{off,i}$.

✓Calculate the **mean value** of $\phi_{off,i}$.







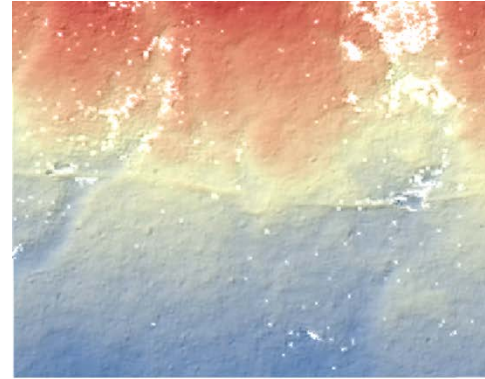
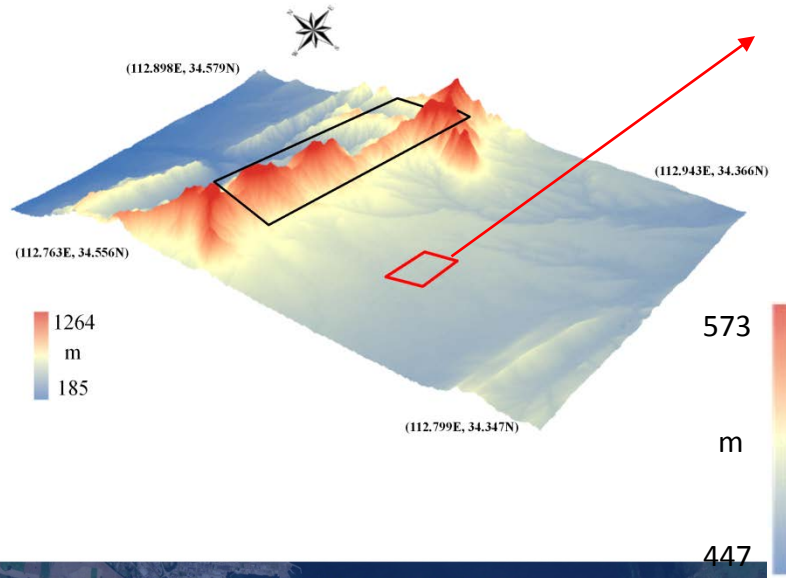
- Mount Song in Henan province of central China;
- The elevation ranges from 150 m to 1500 m above sea level, and the slopes in the central part are very steep;
- Densely vegetated;

ID	Acquisition Mode	Acquisition Date	Orbit Direction	Incidence Angle (°)	Resolution rg/az* (m)
0712	Stripmap	2011-07-12	Ascending	44.5	1.8/3.3
0718	Stripmap	2011-07-18	Ascending	28.9	1.2/3.3
0729	Stripmap	2011-07-29	Ascending	28.9	1.2/3.3

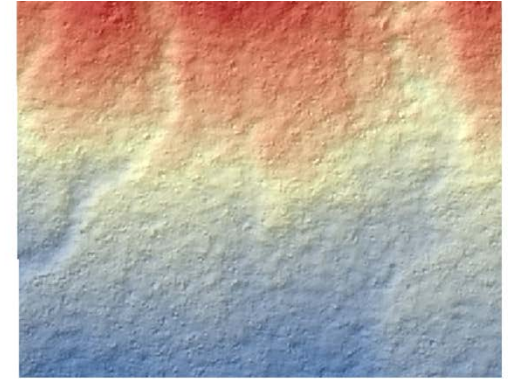
Photogrammetric DSM with spatial resolution of **1 m** has been used as **reference DSM** to evaluate the accuracy of the generated DSM.

Interferometric pair	0718-0729
Temporal baseline	11 d
Normal baseline	194 m
Height ambiguity	22 m

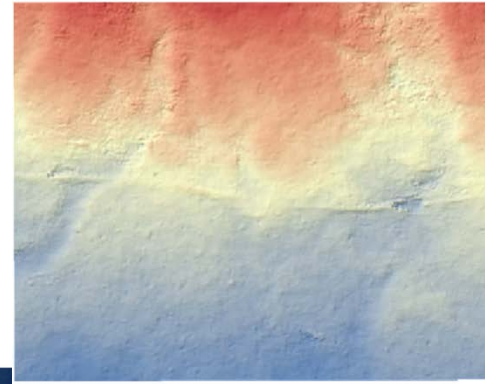
Accuracy evaluation of generated DSMs



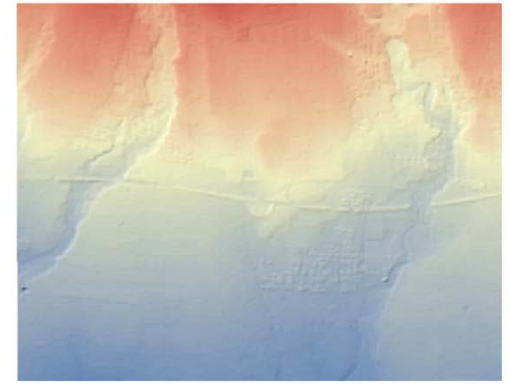
(a) InSAR DSM



(b) StereoSAR DSM

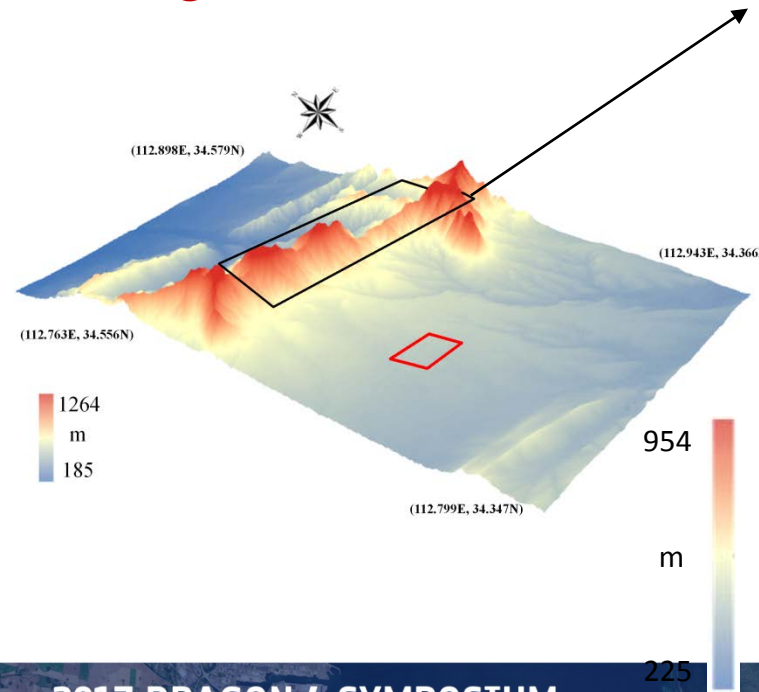


(c) Generated DSM

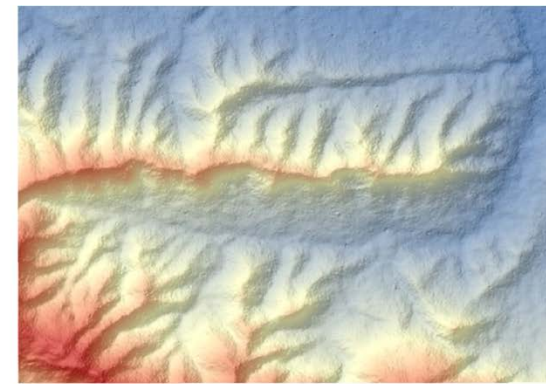


(d) Photogrammetric DSM

Accuracy evaluation of generated DSMs



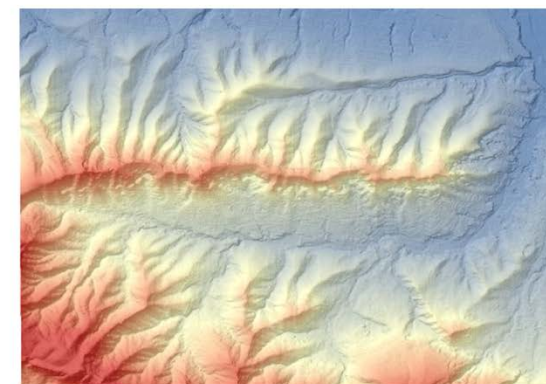
(a) InSAR DSM



(b) StereoSAR DSM



(c) Generated DSM



(d) Photogrammetric DSM

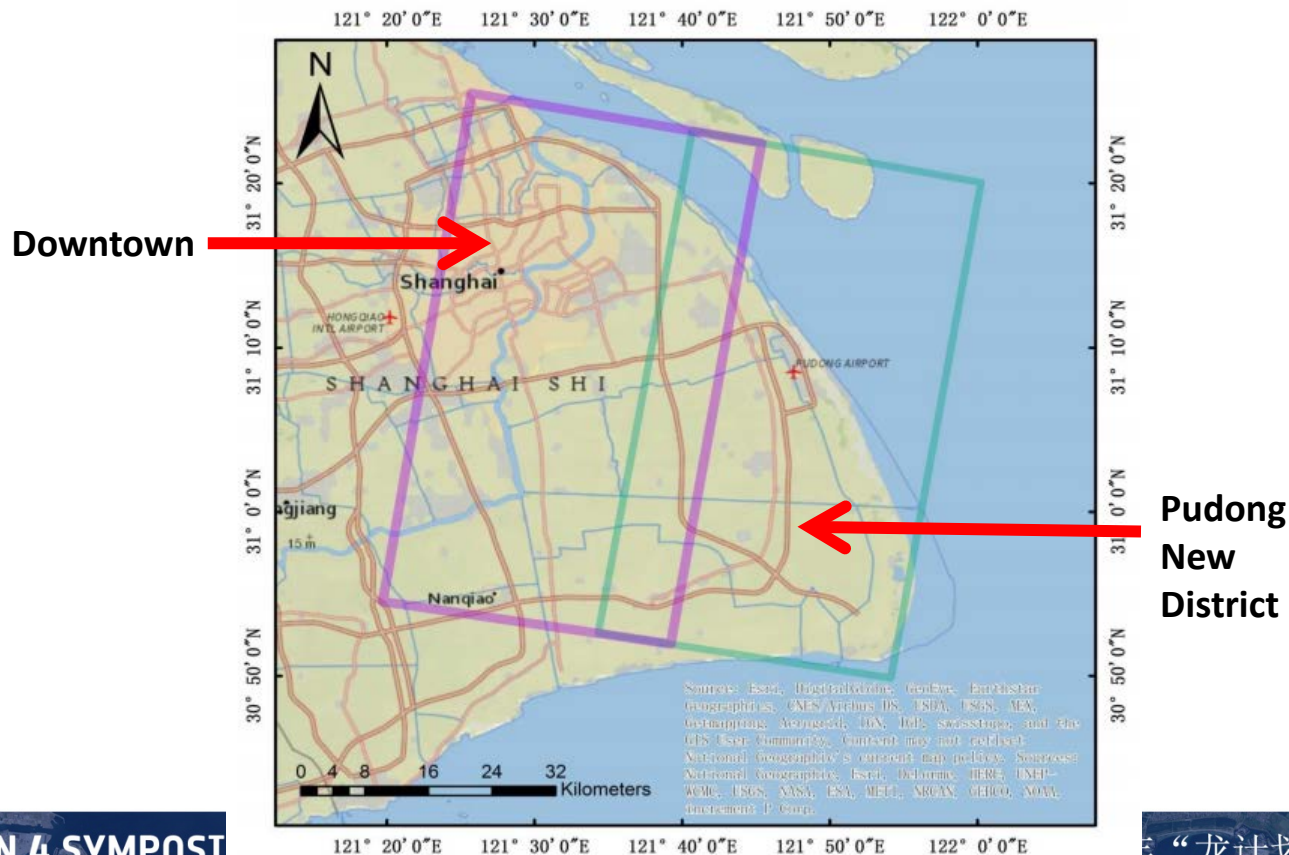
Accuracy evaluation of generated DSMs (m)

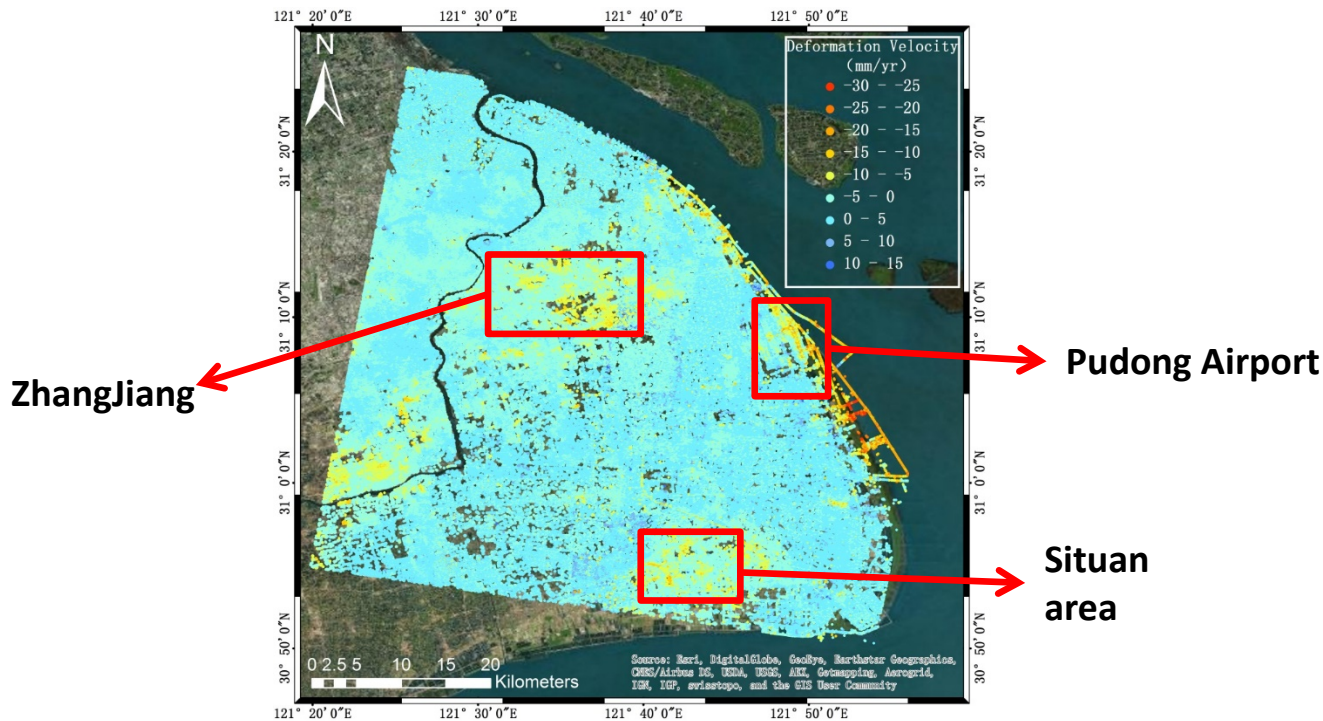
	SRTM DEM			Stereo DSM			generated DSM		
	Mean	RMSE	90% LE	Mean	RMSE	90% LE	Mean	RMSE	90% LE
All	2.7	7.9	13.7	2.5	7.3	12.6	2.3	6.9	11.9
Plains	1.4	2.3	3.9	1.7	1.9	3.3	1.1	1.8	3.2
Mountains	2.6	10.8	18.7	1.7	10.3	17.8	0.9	9.9	17.2

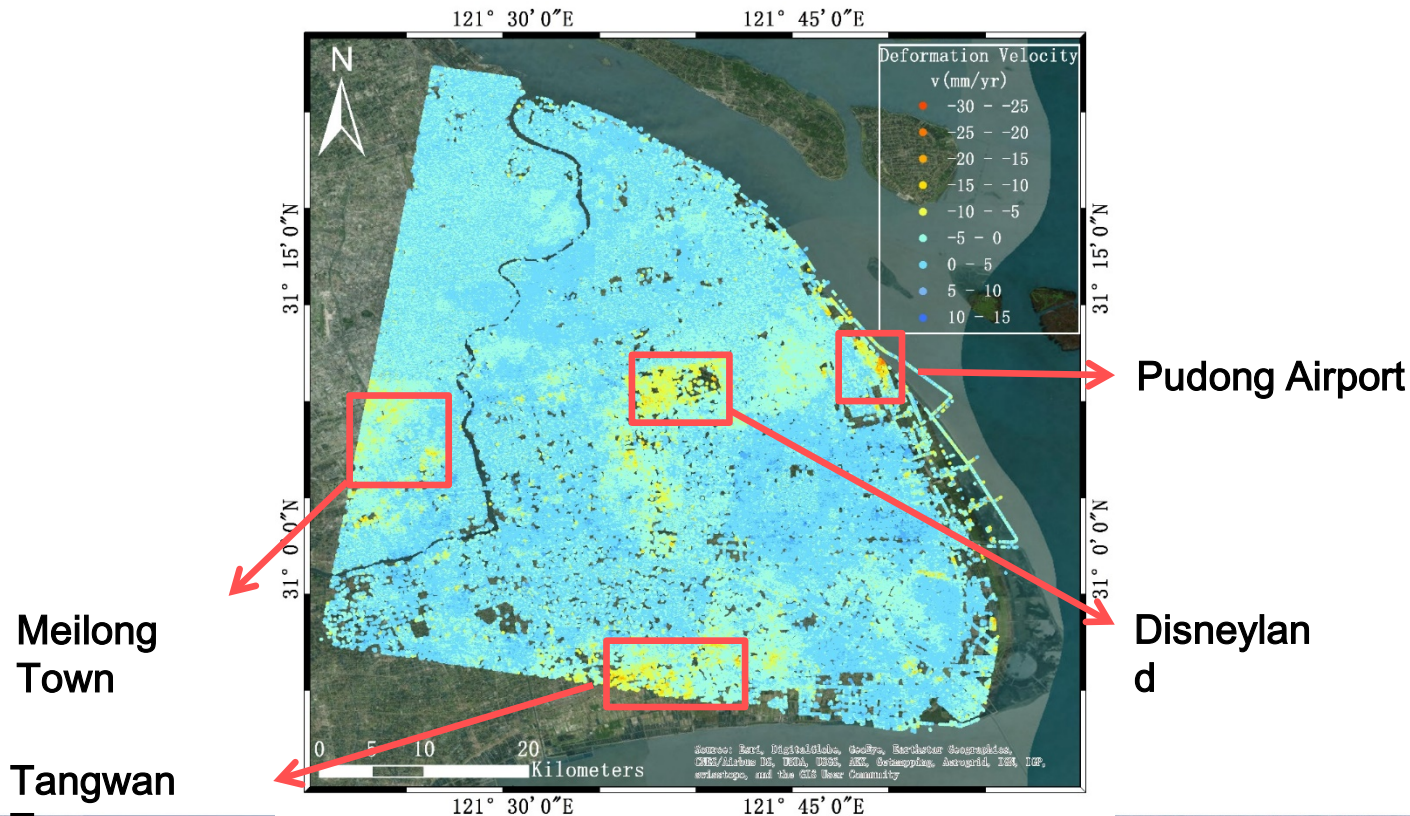
- ✓The AW-LSM algorithm is effective for stereo image matching in mountainous areas with serious geometric distortions.
- ✓Since StereoSAR takes use of the amplitude information, it can be a good complement for decorrelated areas of InSAR data.
- ✓The points with high height accuracy in StereoDSM can be automatically selected for InSAR phase calibration.
- ✓The generated DSM has fewer data voids than InSAR DSM and higher height accuracy than StereoDSM.

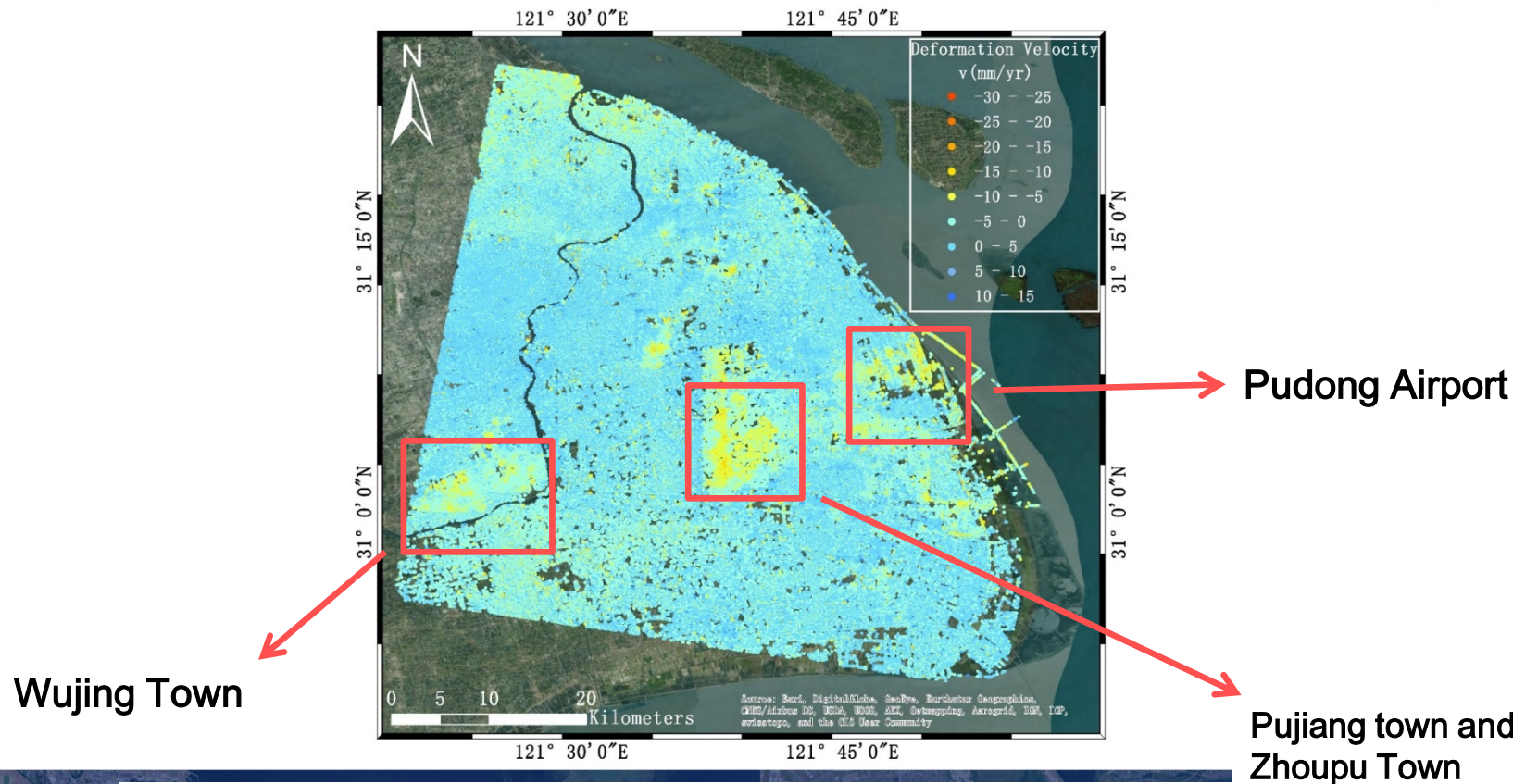
Research activities & Results – Part II

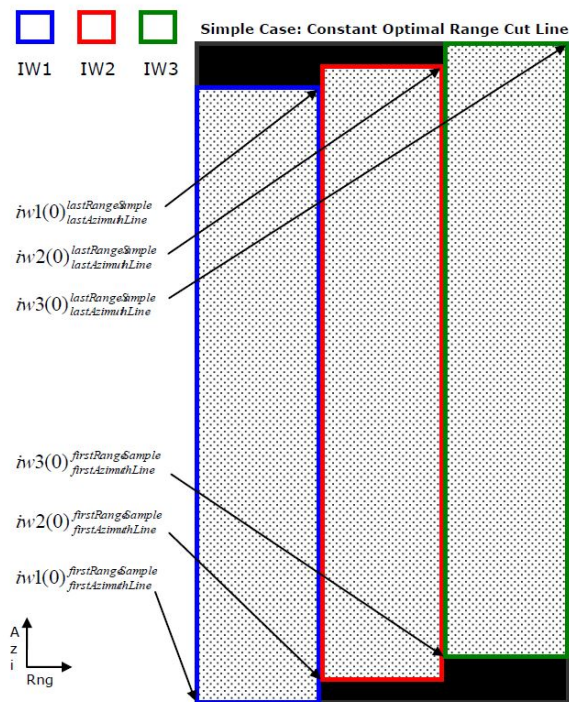
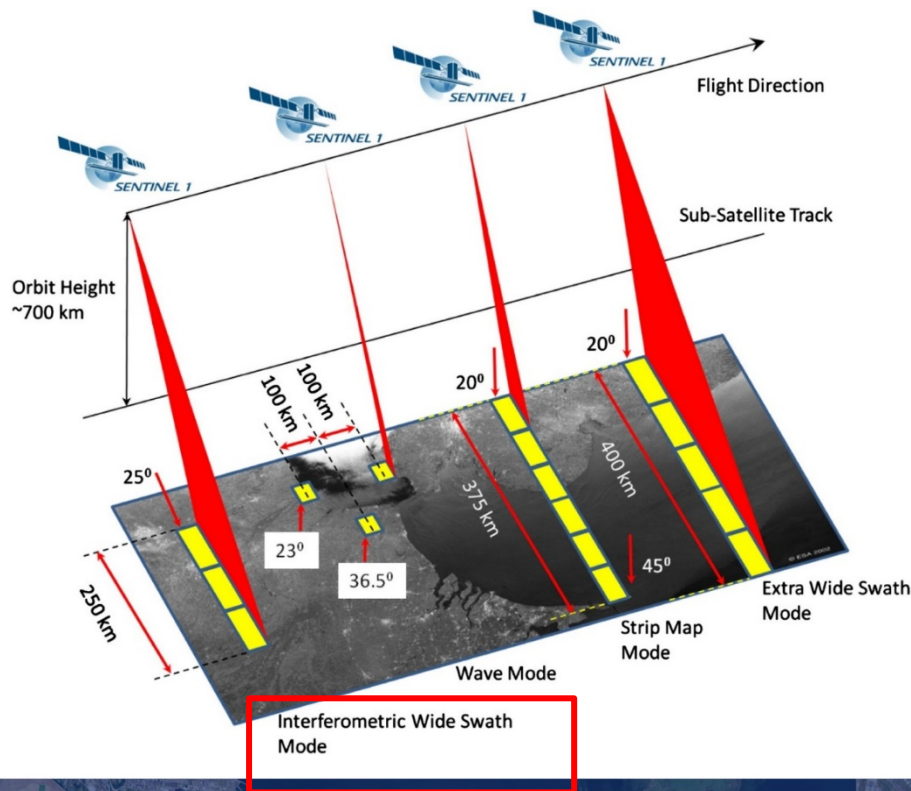
Monitoring subsidence and structure health of infrastructures

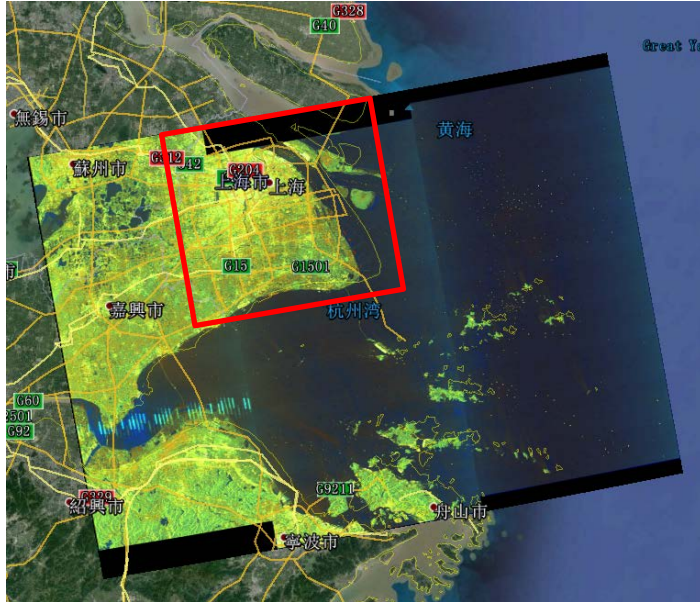












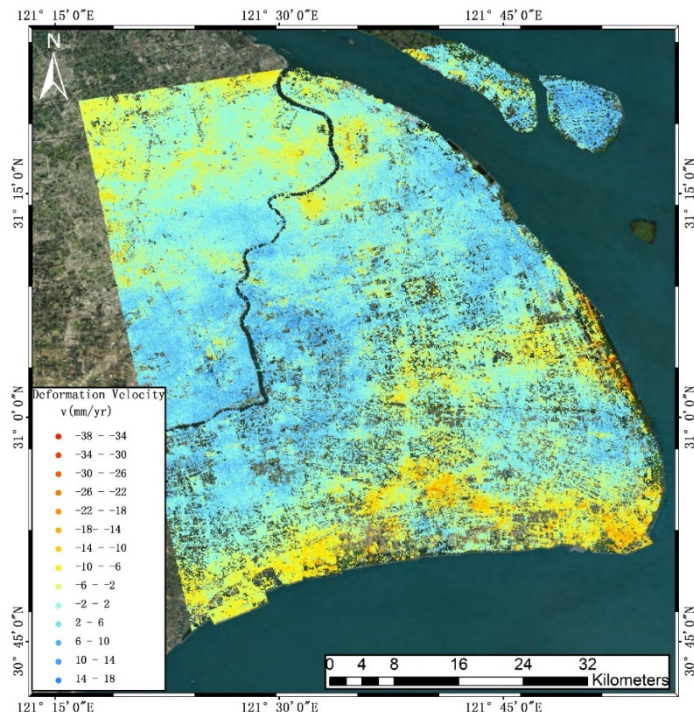
Data coverage

Shanghai subsidence

Pass:
Ascending

archives:
21 images

Dates:
2015-07-08~2016-10-30

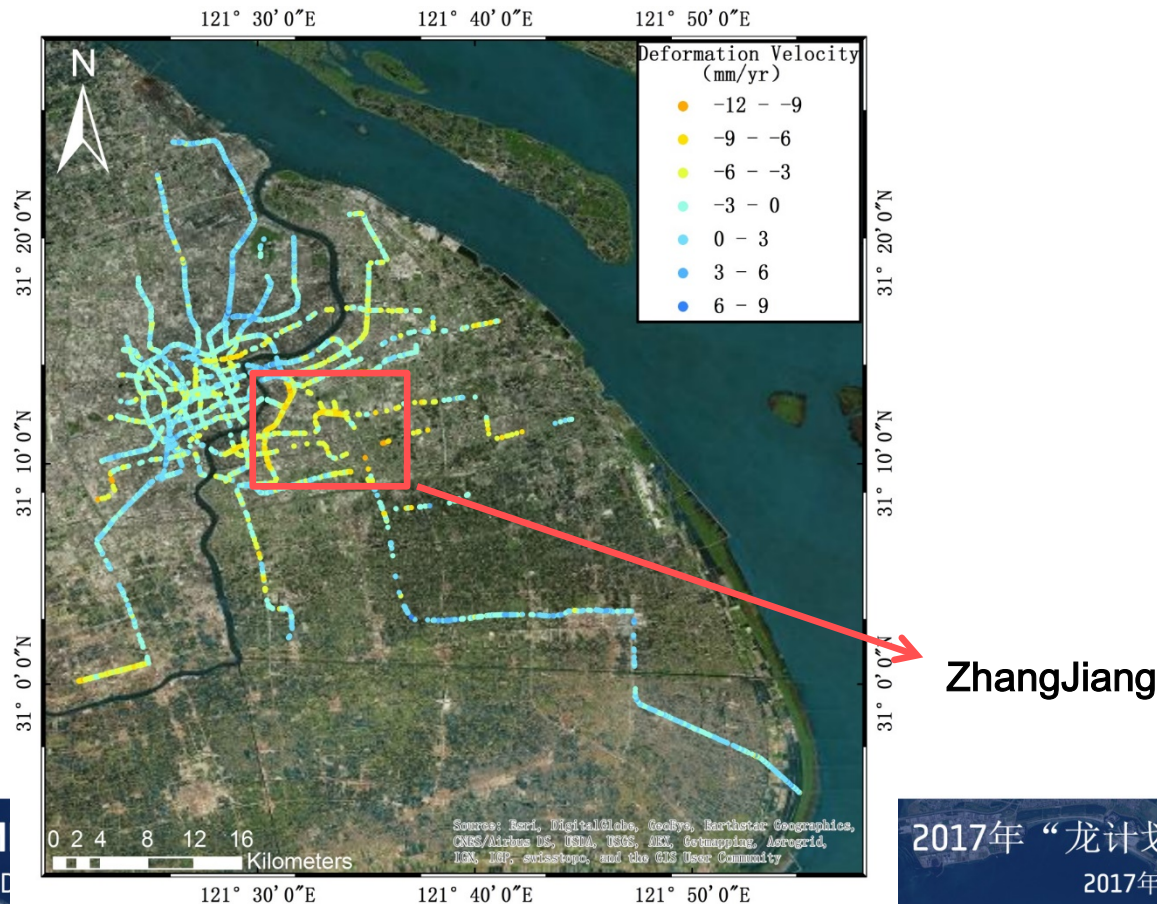


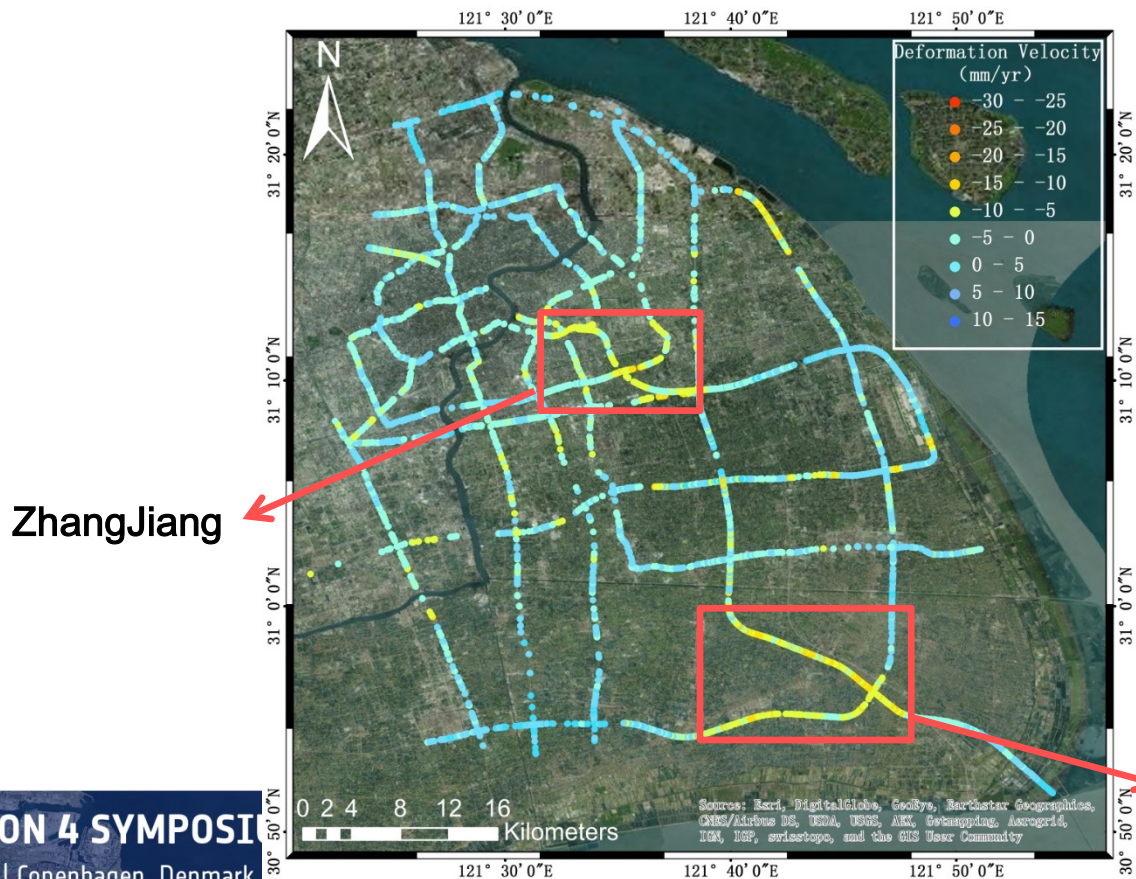
Shanghai subsidence

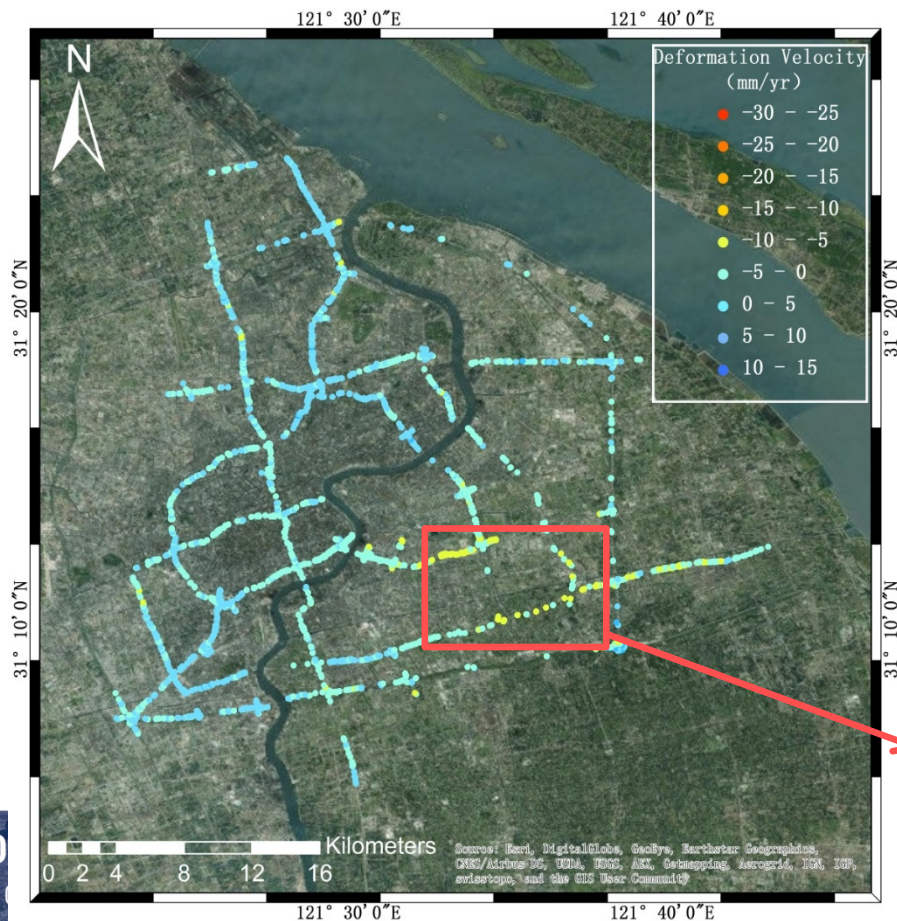
Pass:
Ascending

archives:
15 images

Dates:
2015-07-08~2016-07-26







Elevated roads are more stable except a few sections within ZhangJiang settlement area

ZhangJiang

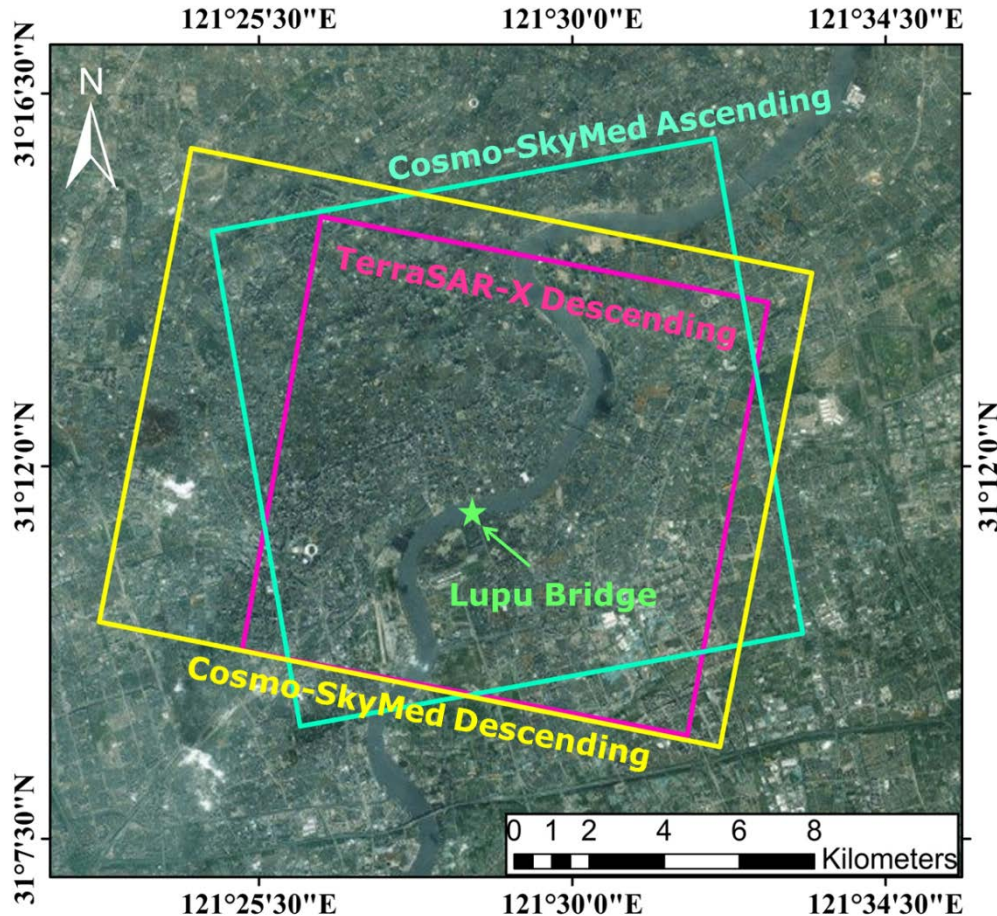
The second longest span of steel arch bridge in the world

Take the main transportation tasks in and out of the Shanghai Expo Park

Famous Landmark in Shanghai



Lupu Bridge - Datasets



- *Lupu Bridge*

- 550 m
- Built:2000/10-2003/06

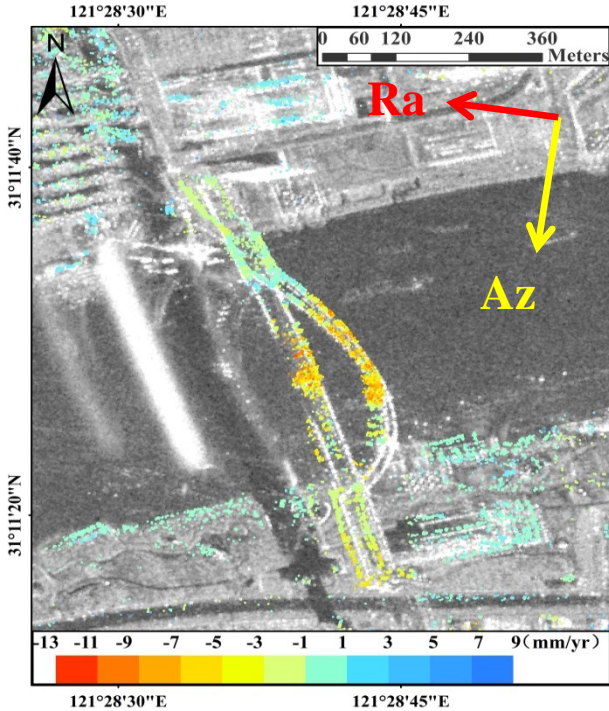
- *TerraSAR-X*

- 18 descending images
- 2009/03-2010/01

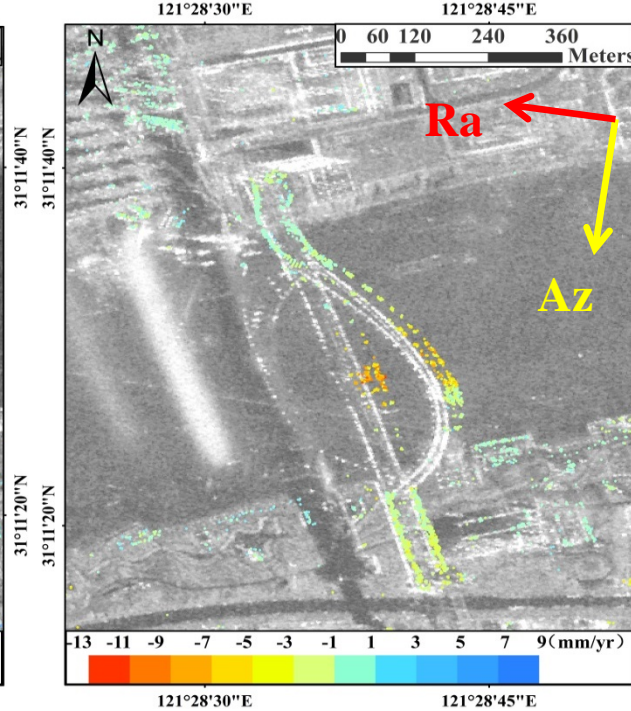
- *Cosmo-SkyMed*

- 18 descending & ascending images
- 2009/02-2010/01

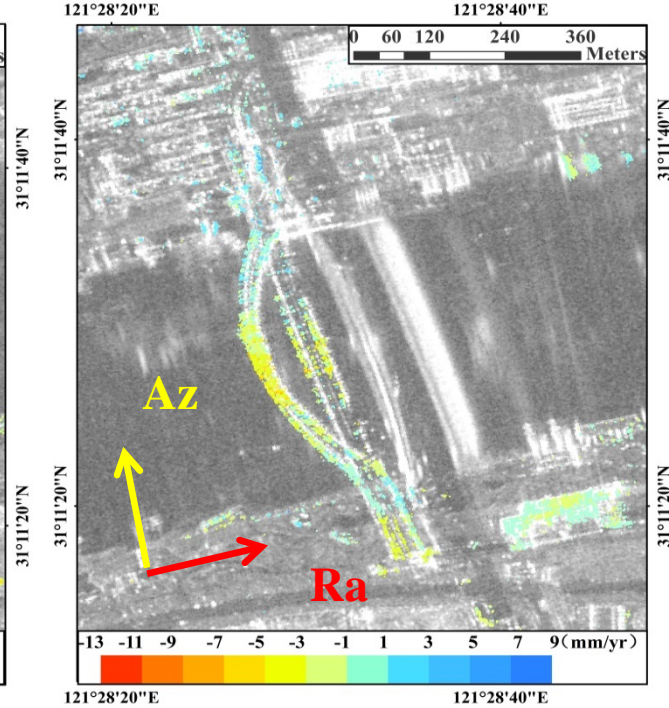
TerraSAR-X (Desc)



Cosmo-SkyMed (Desc)



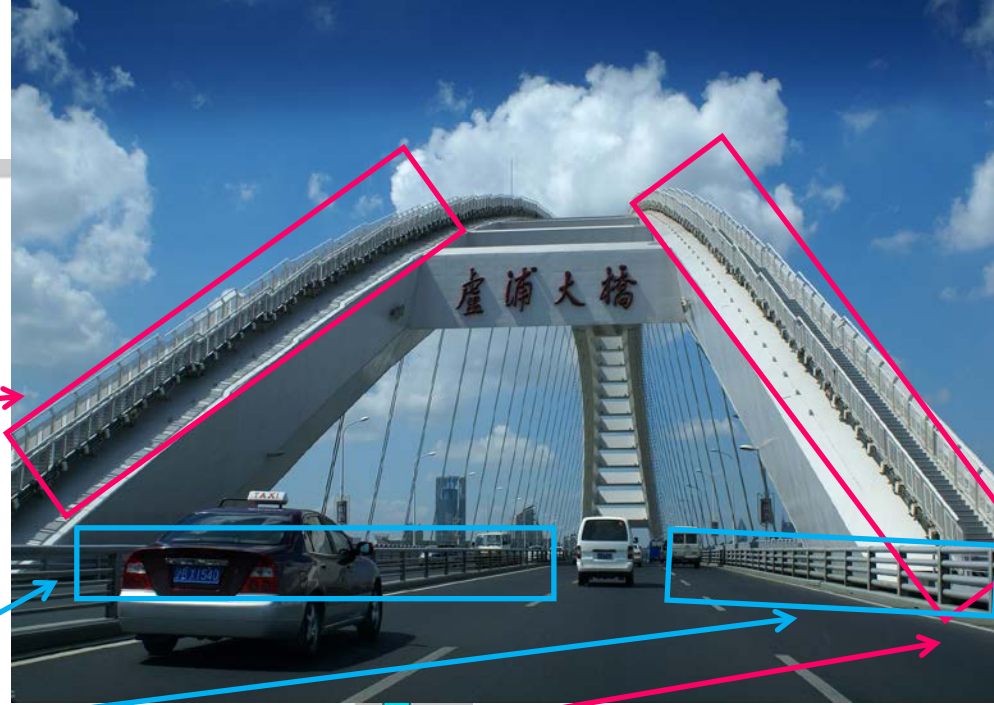
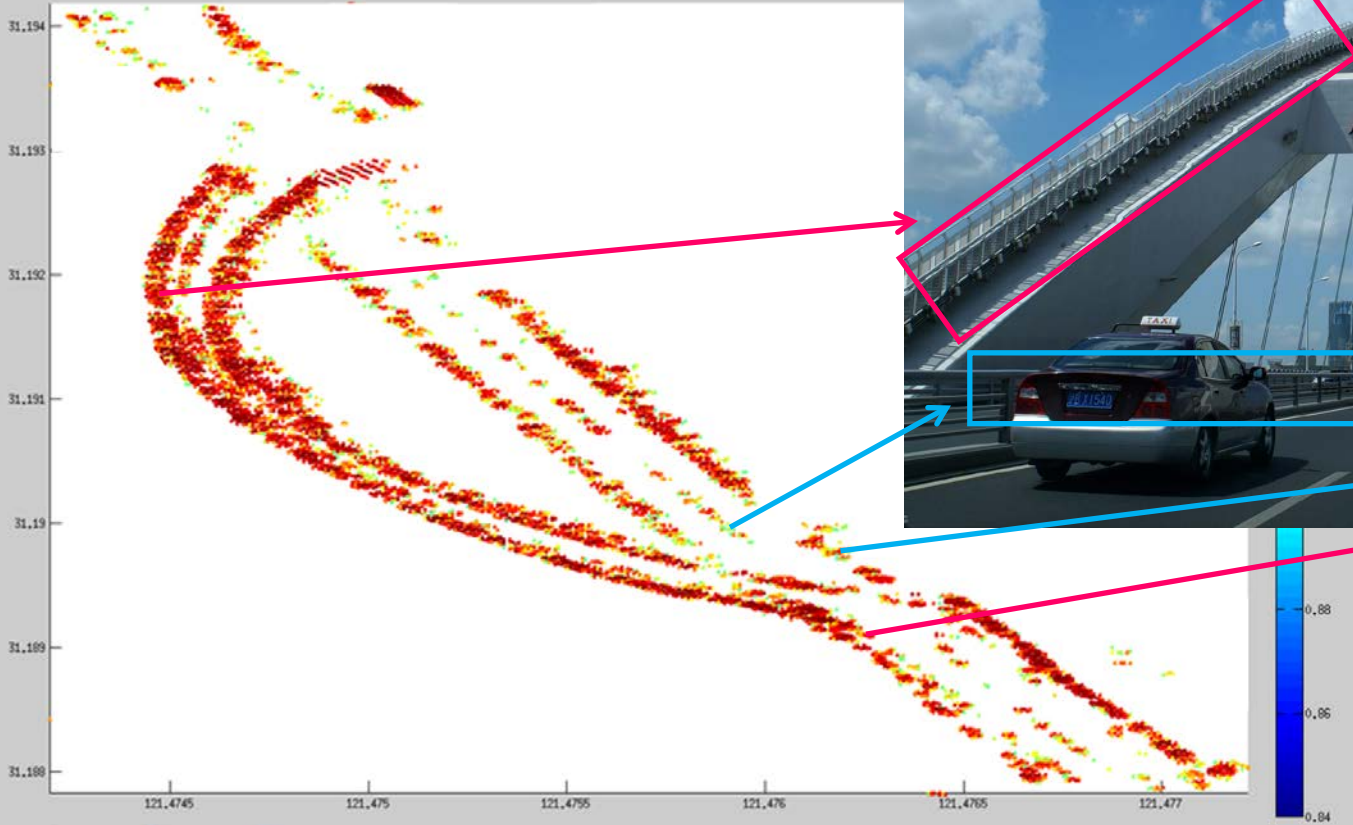
Cosmo-SkyMed (Asc)



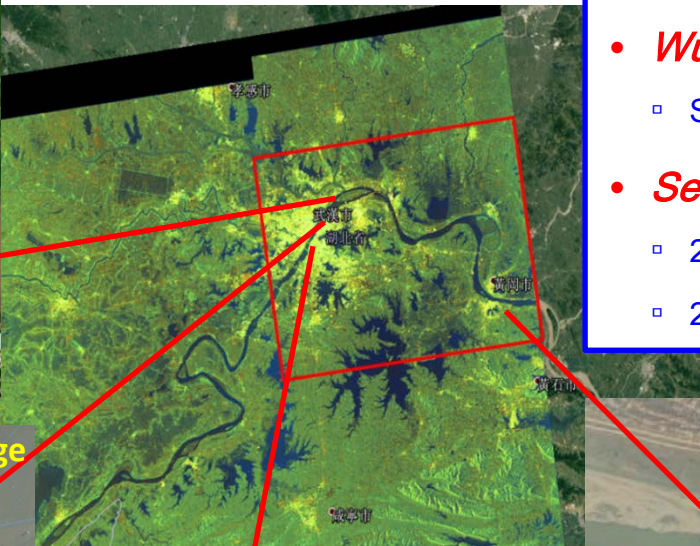
The same deformation patterns

Different incidence angles and acquisition dates lead to a little difference in LOS displacements

PTs Distribution

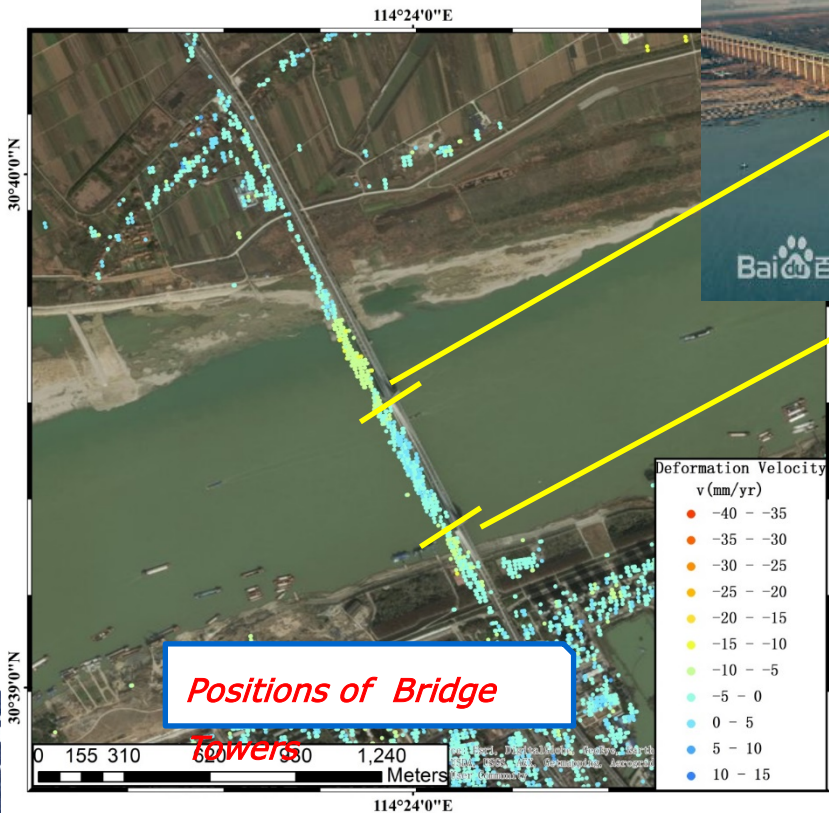


PTs on the Arch
 PTs on the beam
 All from the railings



- *Wuhan*
 - Shown as red box
- *Sentinel-1*
 - 23 images
 - 2015/04-2016/11





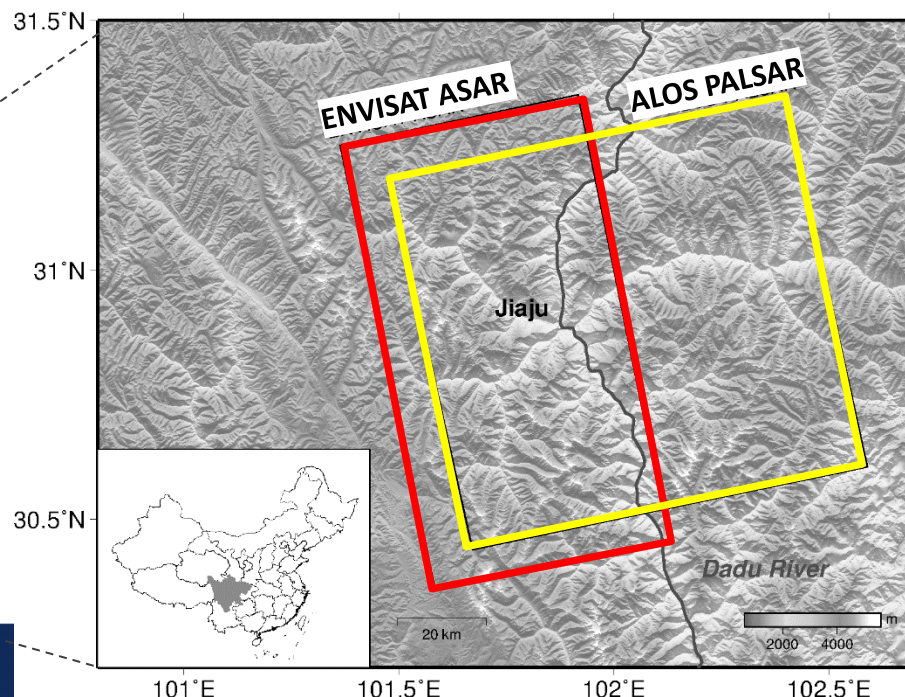
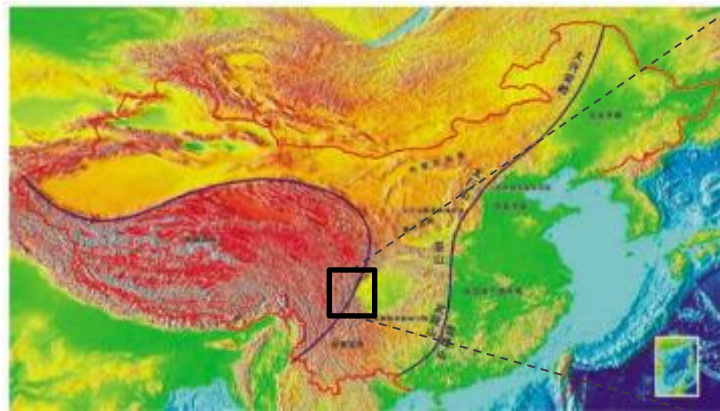
- *Wuhan*
 - Tianxingzhou Bridge
 - Built:2004/09-2008/09

Research activities & Results – Part III

Landslide Displacement Monitoring by InSAR Analyses with Persistent and Distributed Scatterers

Case Study of Danba County, China

- The zone of first step extending to second step of the China's three ladders
- The upper reach of Dadu River in Danba County, West of China
 - **Steep and forested terrains**
 - **Active tectonic movements**
 - **Frequent geological hazards**

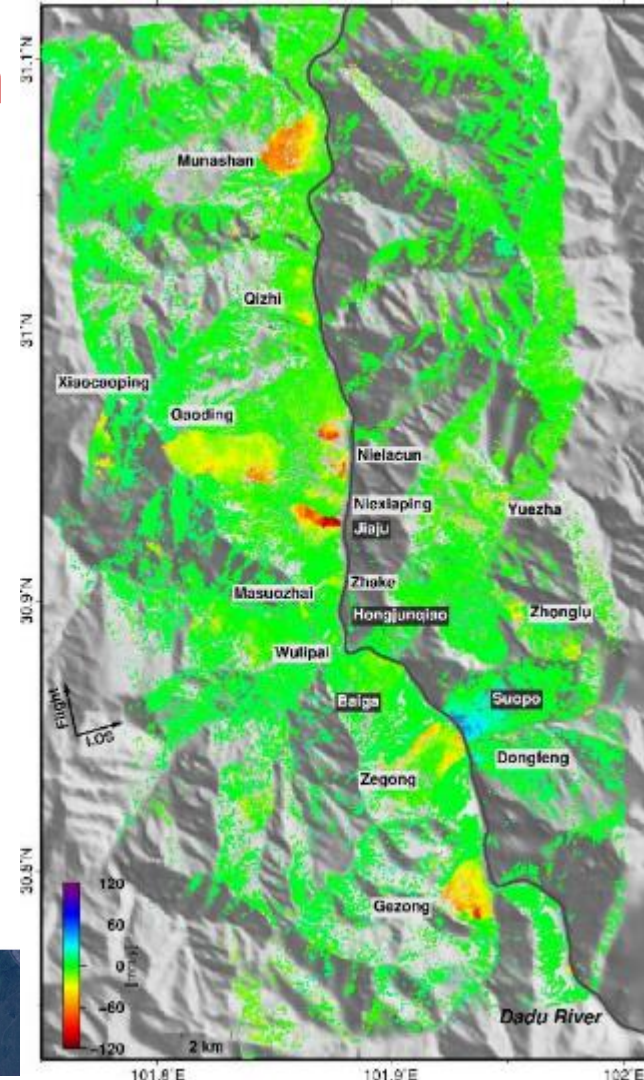


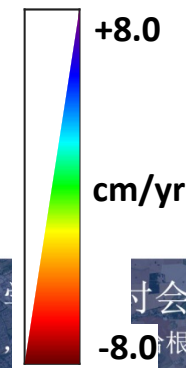
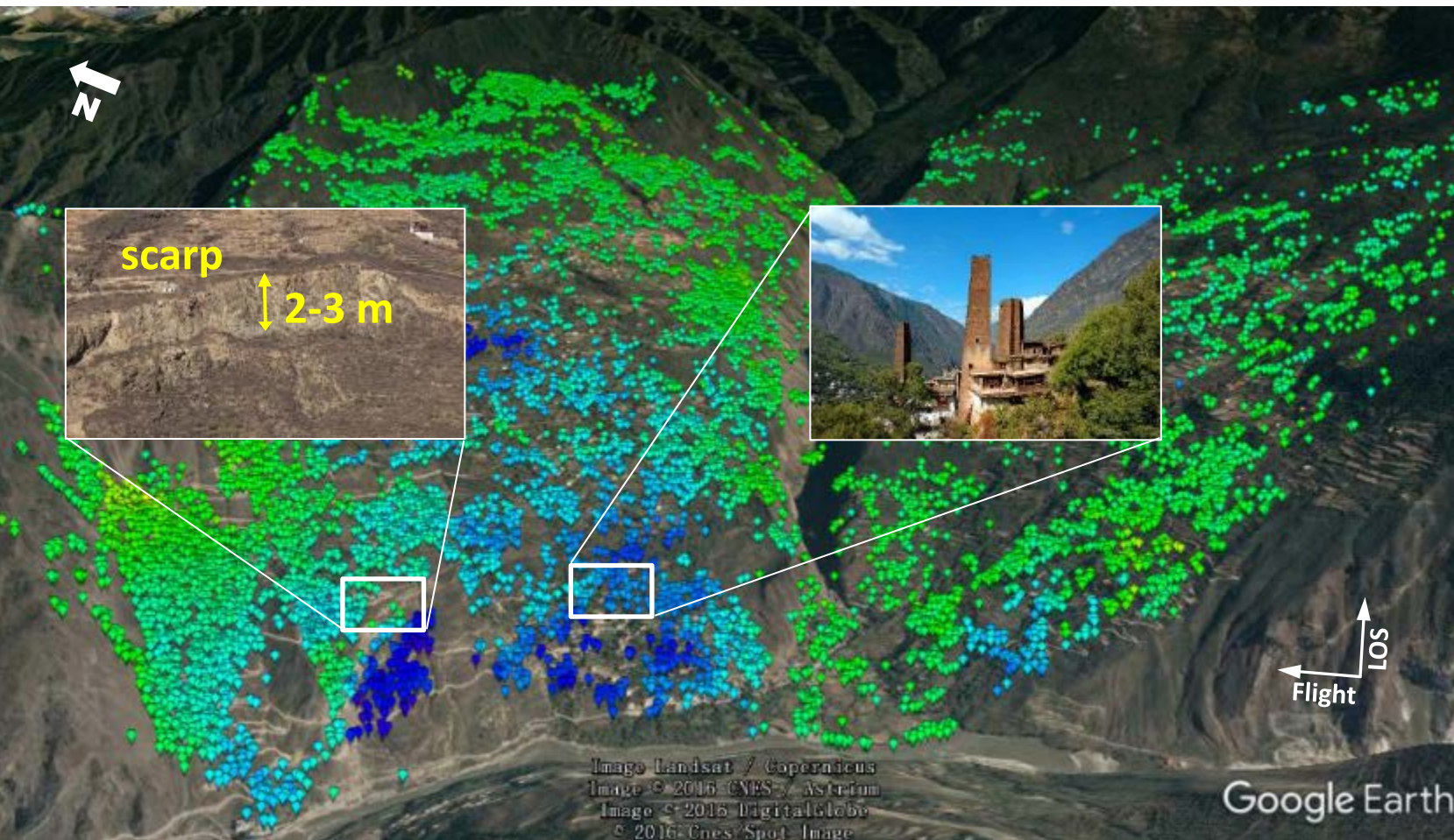
LOS deformation rate map derived by **DSI** from **PALSAR** (2006-2011)

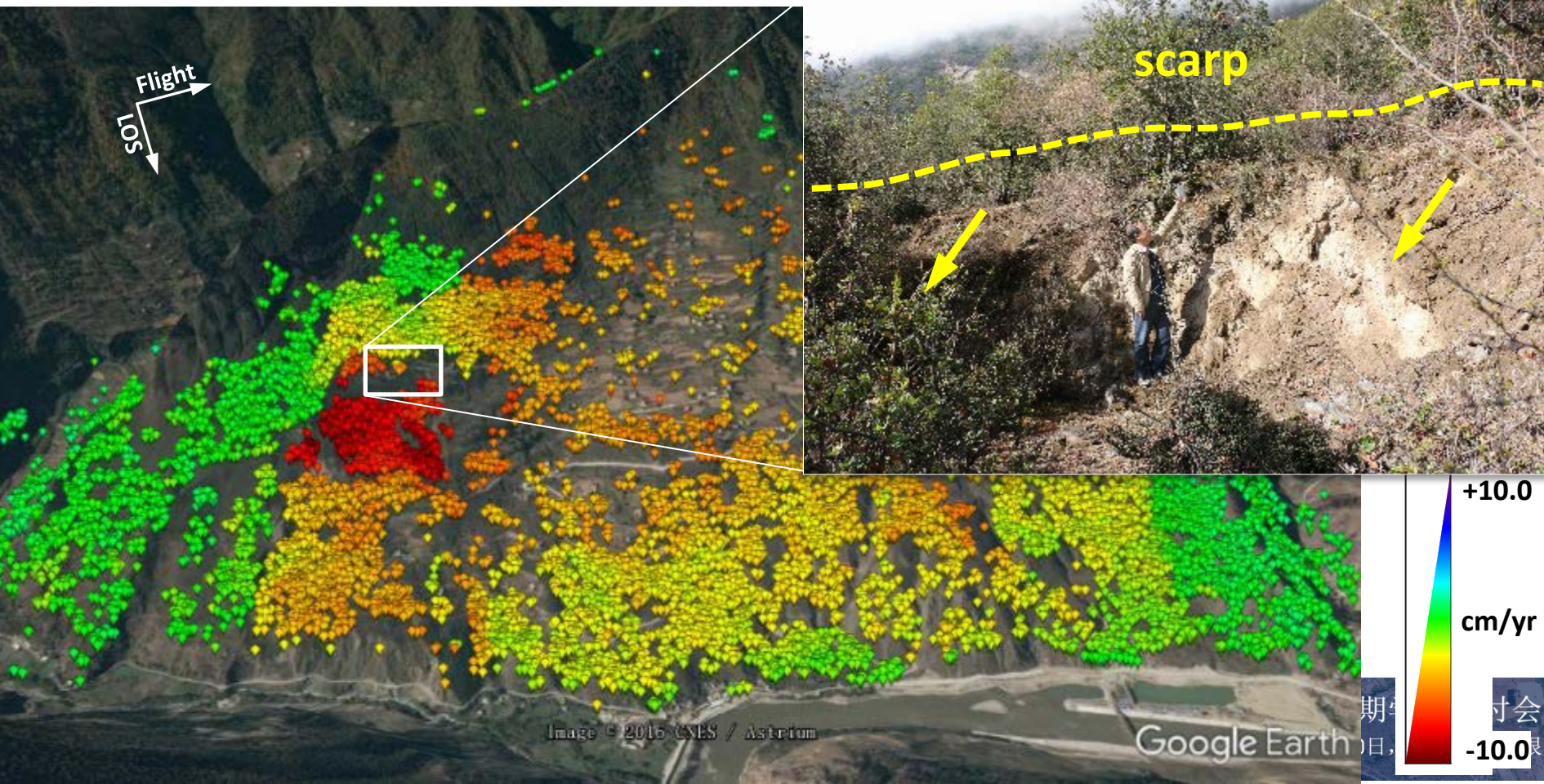
- More than **4,000,000** measurement points (MPs) identified over an area of 1,000 km²
- A spatial density of over **4,000 MPs/km²**
- **16 landslides** detected along the Dadu River

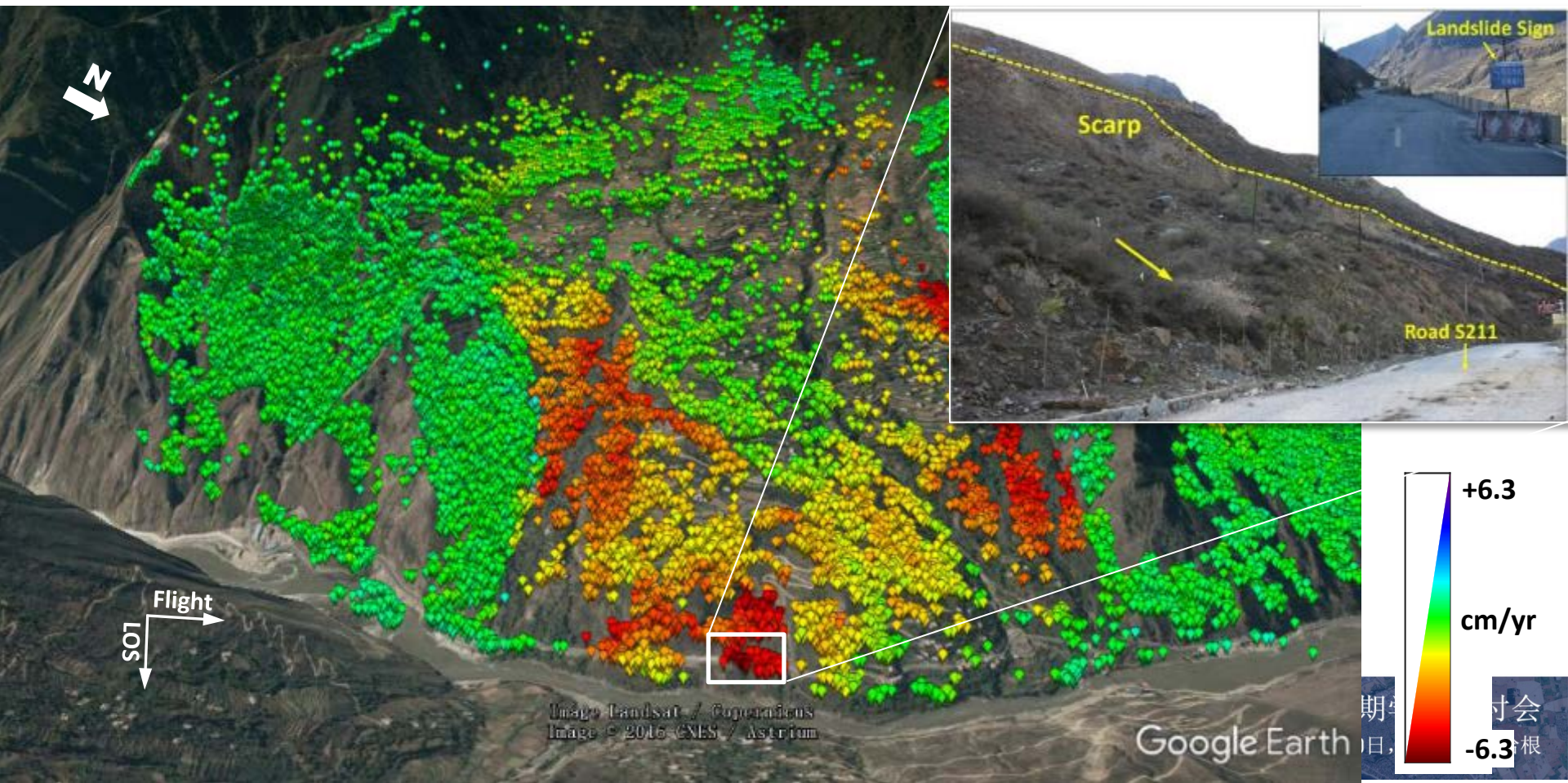


field survey

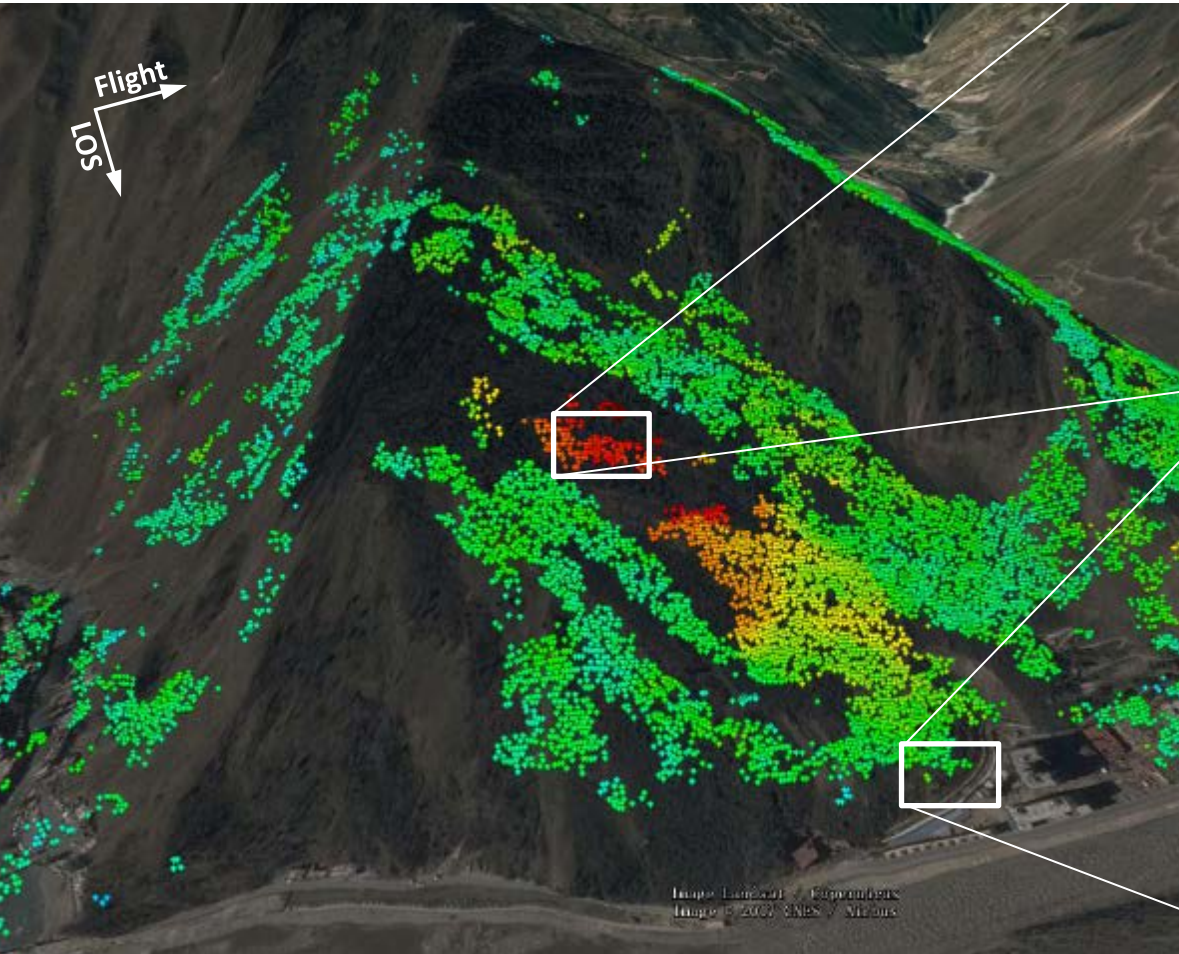








Results – Wulipai landslide

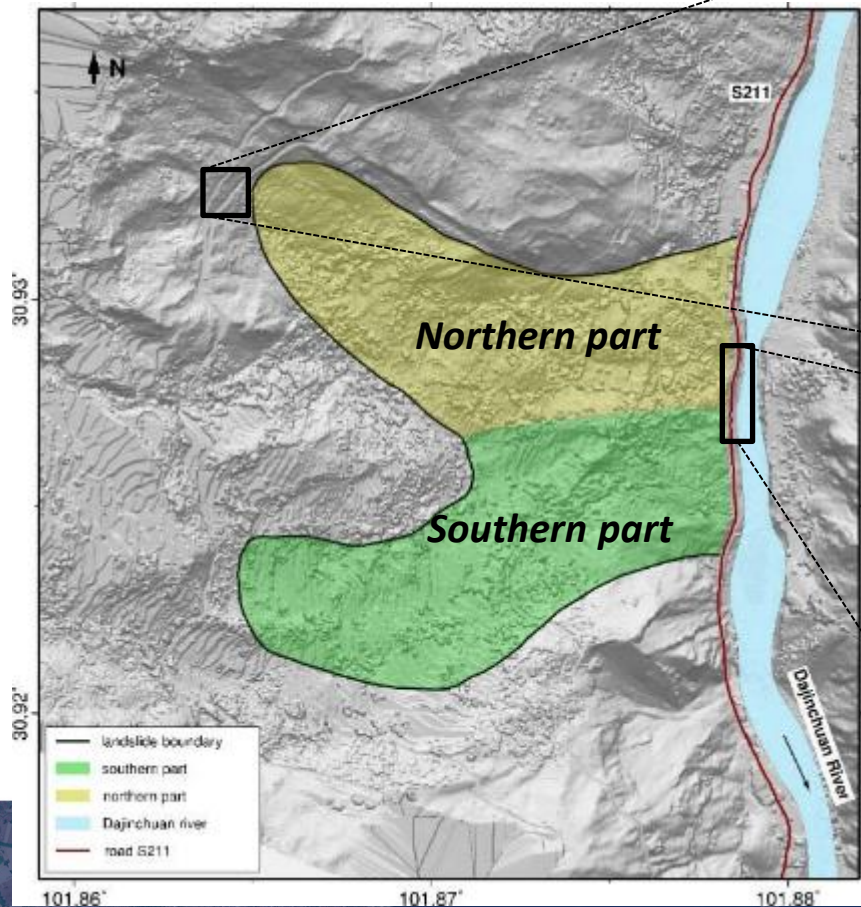




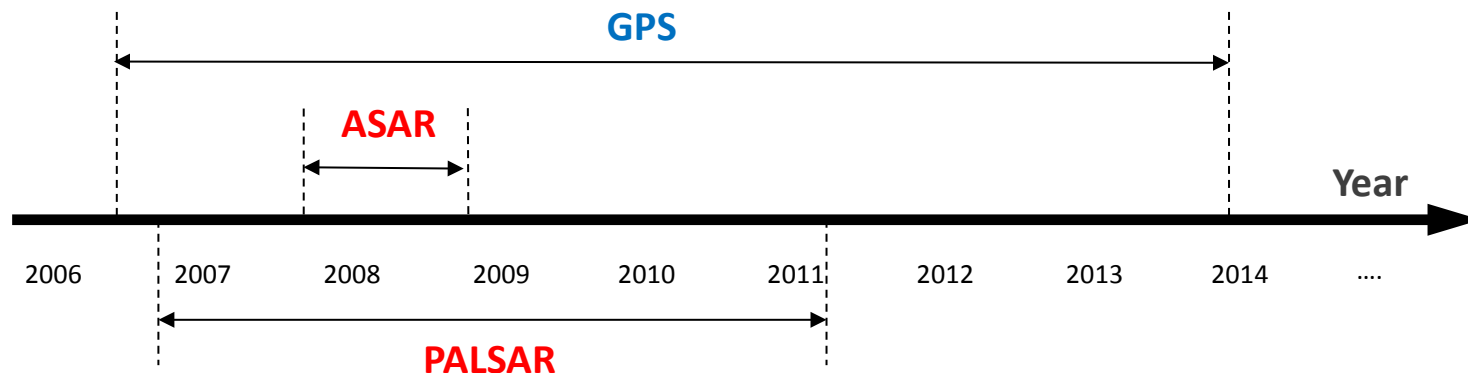
Jiaju Village

- A well-known Tibetan style village
- One of the most beautiful villages in China

Study Area - Jiaju landslide



- Two
- Roa



SAR images:

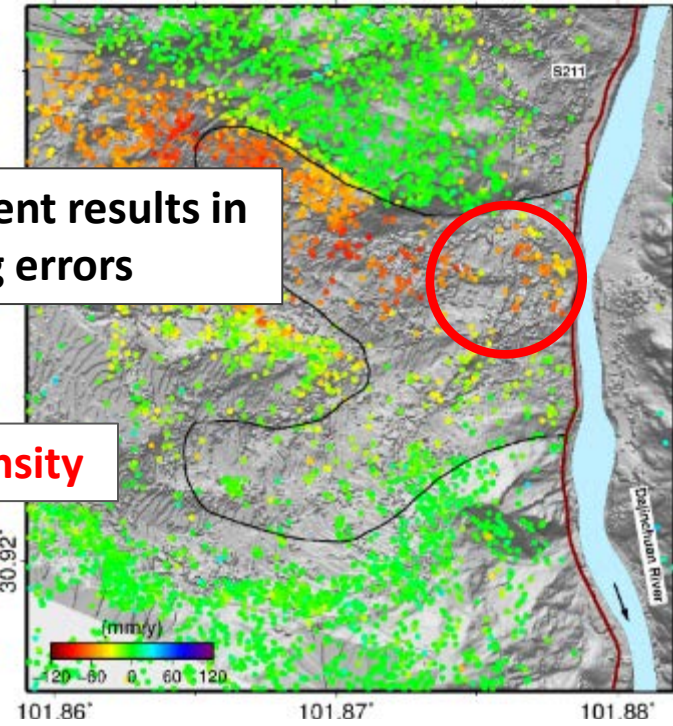
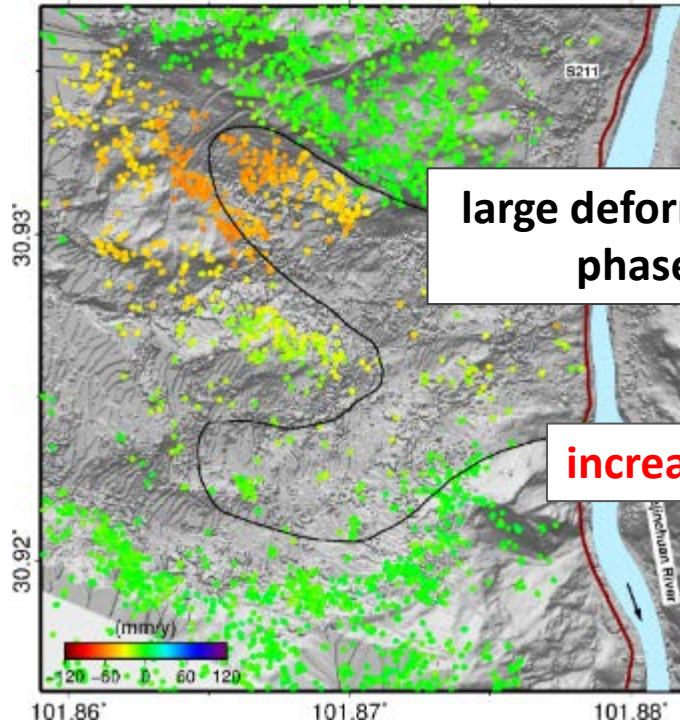
- L-band ALOS PALSAR: Ascending, 19 images, Dec-2006 - Jan-2011
- C-band ENVISAT ASAR: Ascending, 9 images, Aug-2007 - Jun-2008

GPS observations for Jiaju landslide:

- 20 monitoring + 2 reference stations
- Trimble 5700 GPS receivers
- Aug-2006 – Dec-2013

PSI

SBAS



large deformation gradient results in
phase unwrapping errors



increase points density

DSI method:

**Persistent Scatterers (PS) +
Distributed Scatterers (DS)**

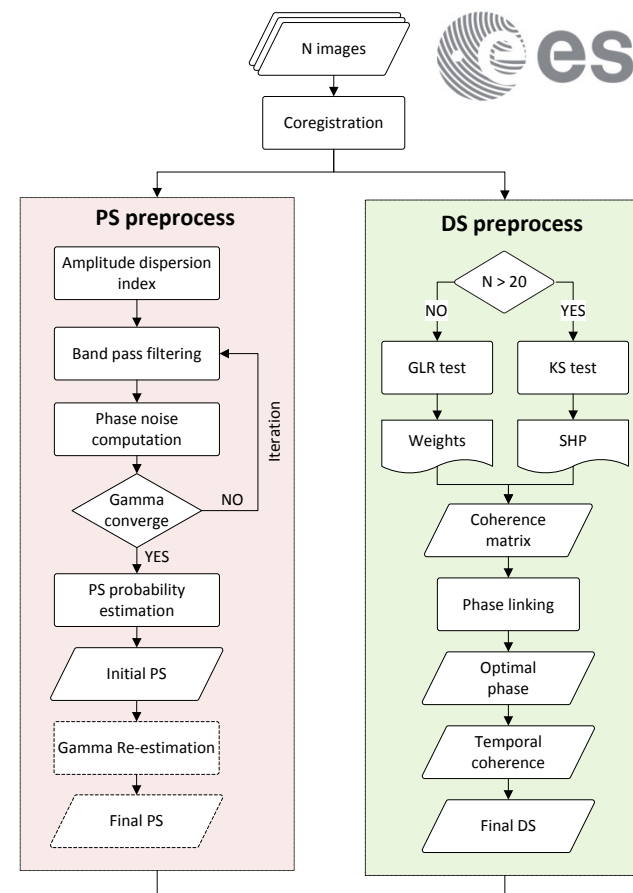
(1) PS preprocessing:

StaMPS/PSInSAR

(2) DS preprocessing

(3) Combination analysis of PS and DS

standard time series analysis

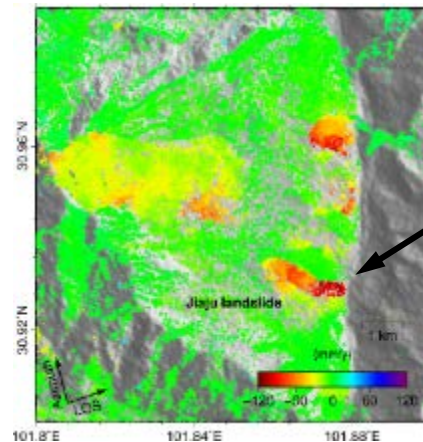
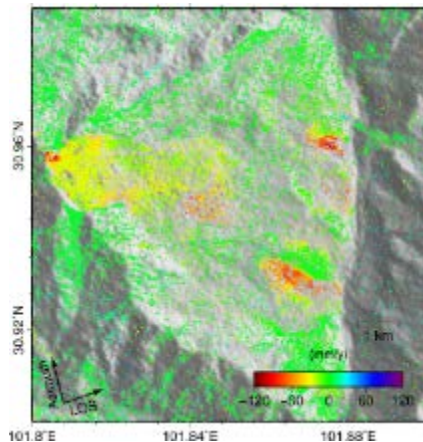
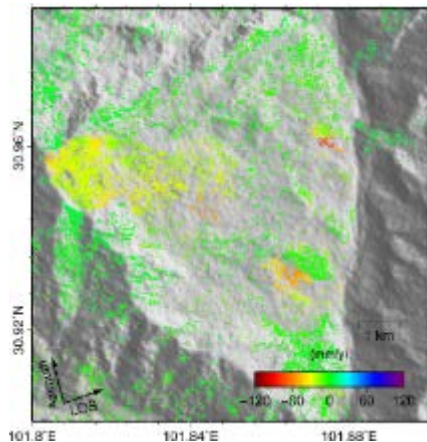


PSI

SBAS

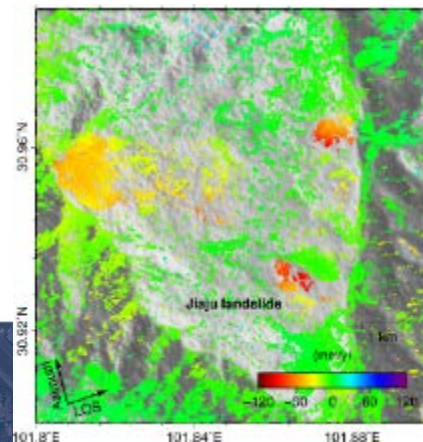
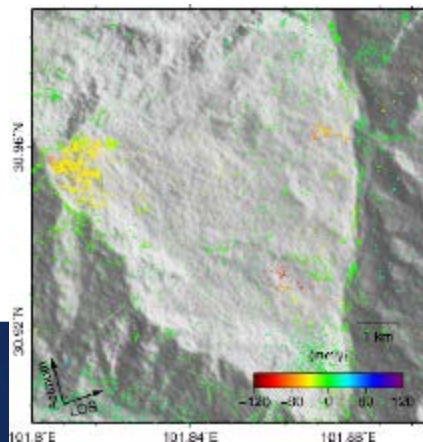
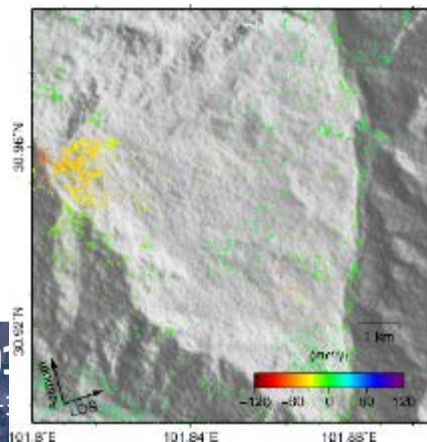
DSI

PALSAR



Jiaju landslide

ASAR



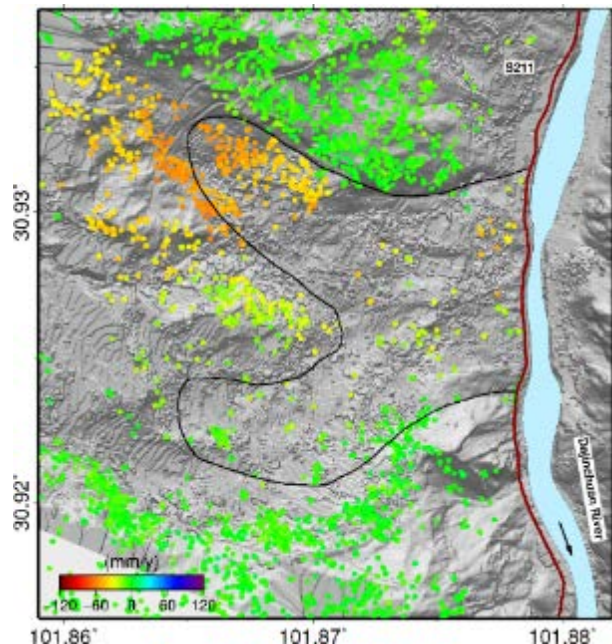
	Spatial density (MPs/km ²)	
	PALSAR	ASAR
PSI	323	44
SBAS	498	107
DSI	4,973	1,093

M

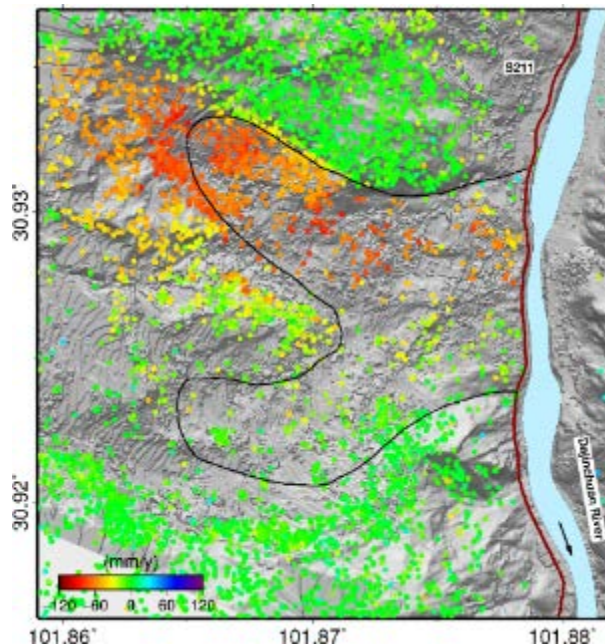
“龙计划” 四期学术研讨会

PSI & SBAS: StaMPS

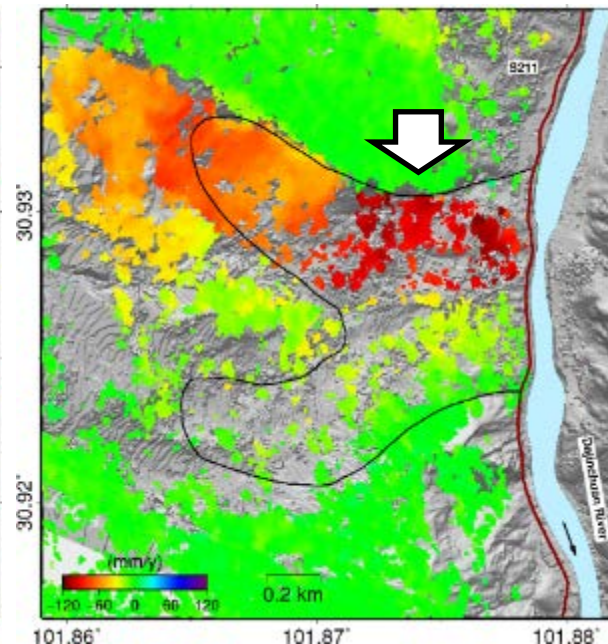
PSI



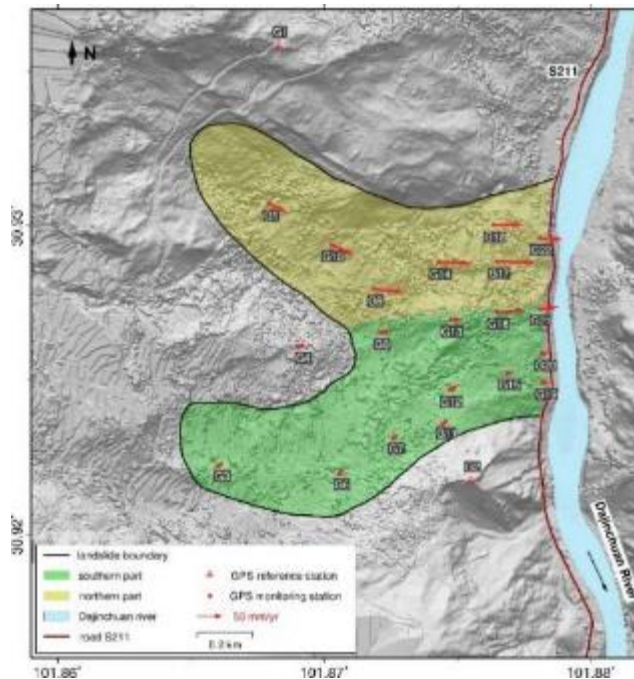
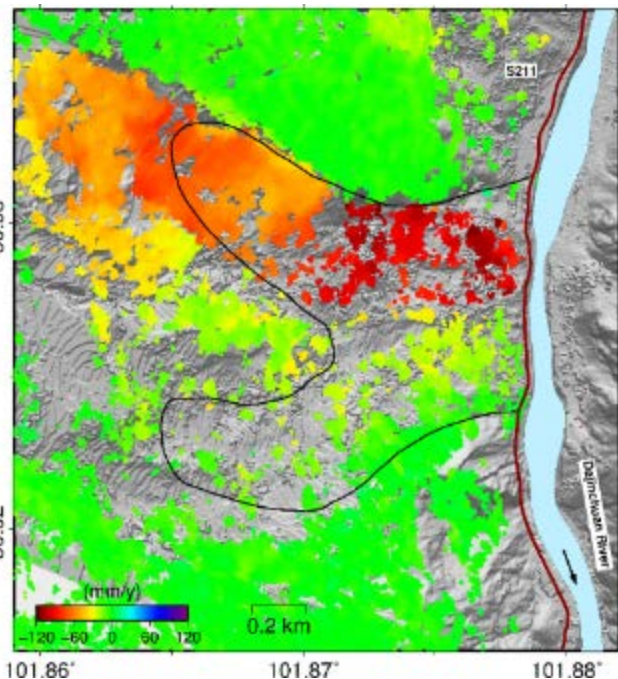
SBAS



DSI



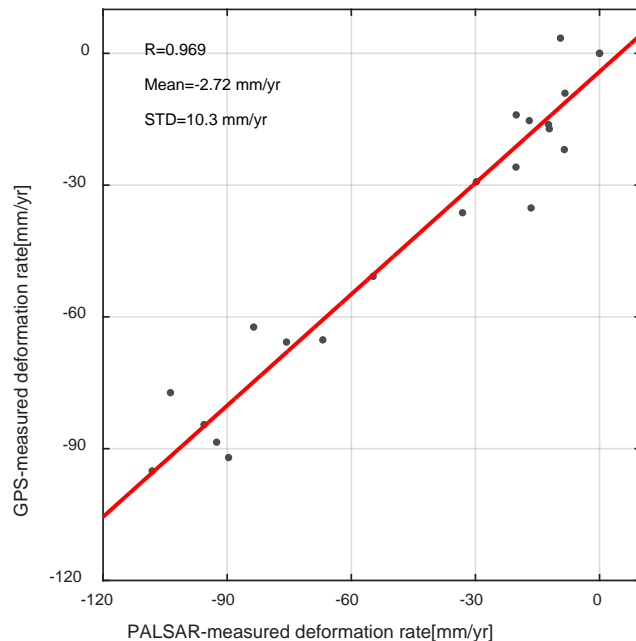
Validation with GPS measurements



- The northern part (120 mm/yr) moved much faster than the southern part
- The foot moved faster than the head
- InSAR results agree well with GPS results

Validation with GPS measurements

GPS rate



- The correlation between DSI-derived PALSAR rate and GPS rate on the GPS stations is **0.96**
- The mean difference is **-2.7** mm/yr
- The STD of the differences is **10.9** mm/yr

DSI-derived PALSAR rate

2017 DRAGON 4 SYMPOSIUM

26-30 June 2017 | Copenhagen, Denmark

2017年“龙计划”四期学术研讨会

2017年6月26-30日, 丹麦 哥本哈根

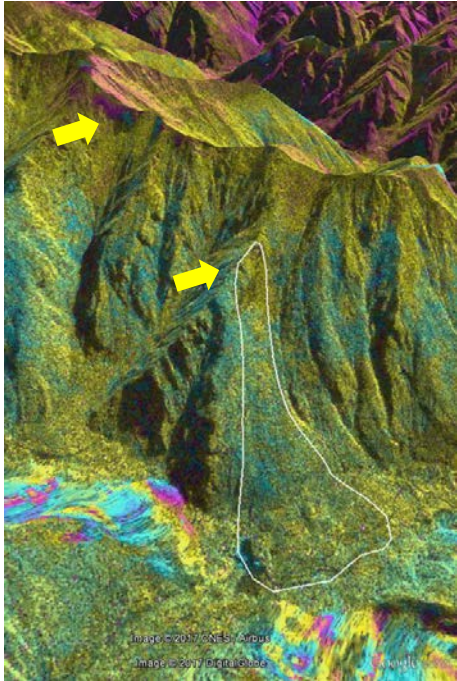
A Large landslide happened in Mao County on the morning of **2017-06-24**

More than 100 people are missing

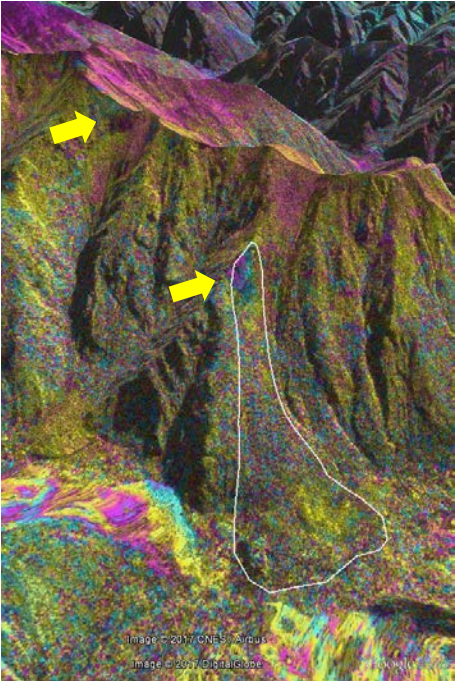


D-InSAR results from ALOS-2 PALSAR-2 data

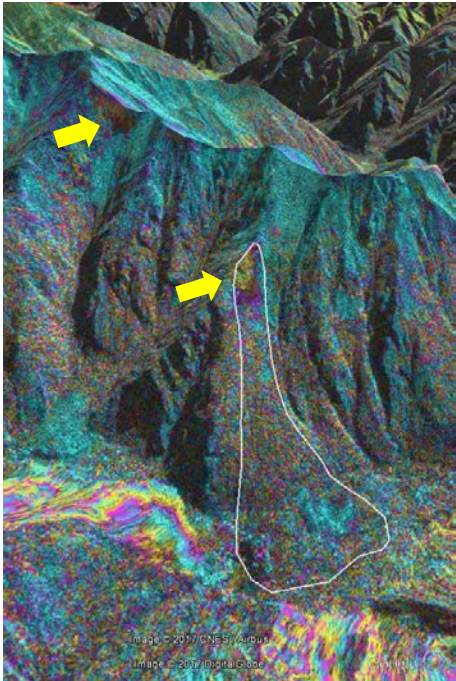
20150606-20150620
14 days, Bp:108m



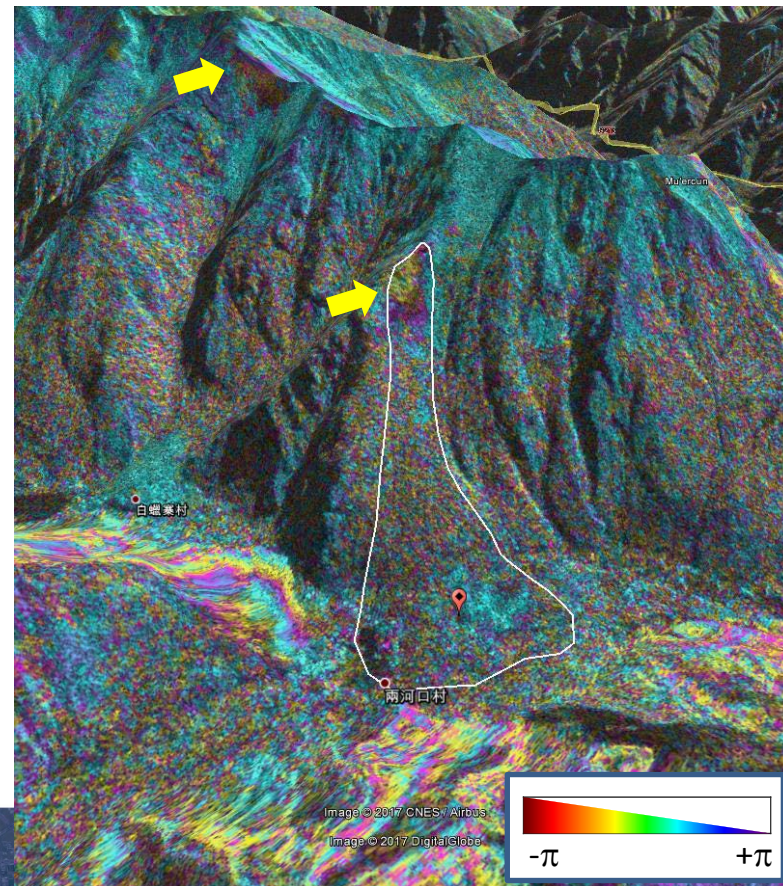
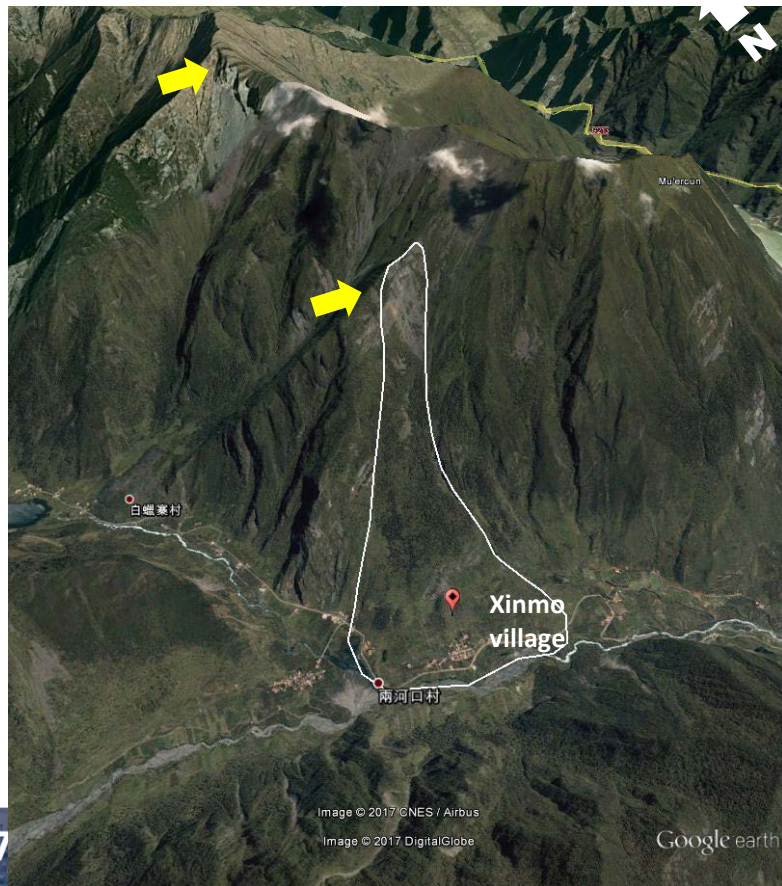
20150606-20170617
742 days, Bp:91m



20150620-20170617
728 days, Bp:199m



20150620-20170617



2017

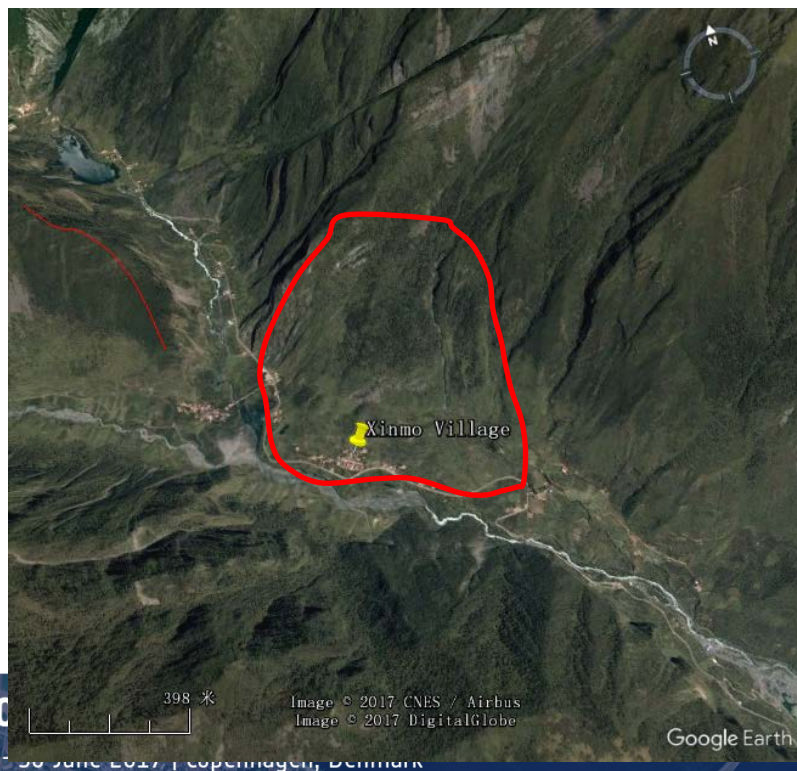
26-30 June 2017 | Copenhagen, Denmark

研讨会

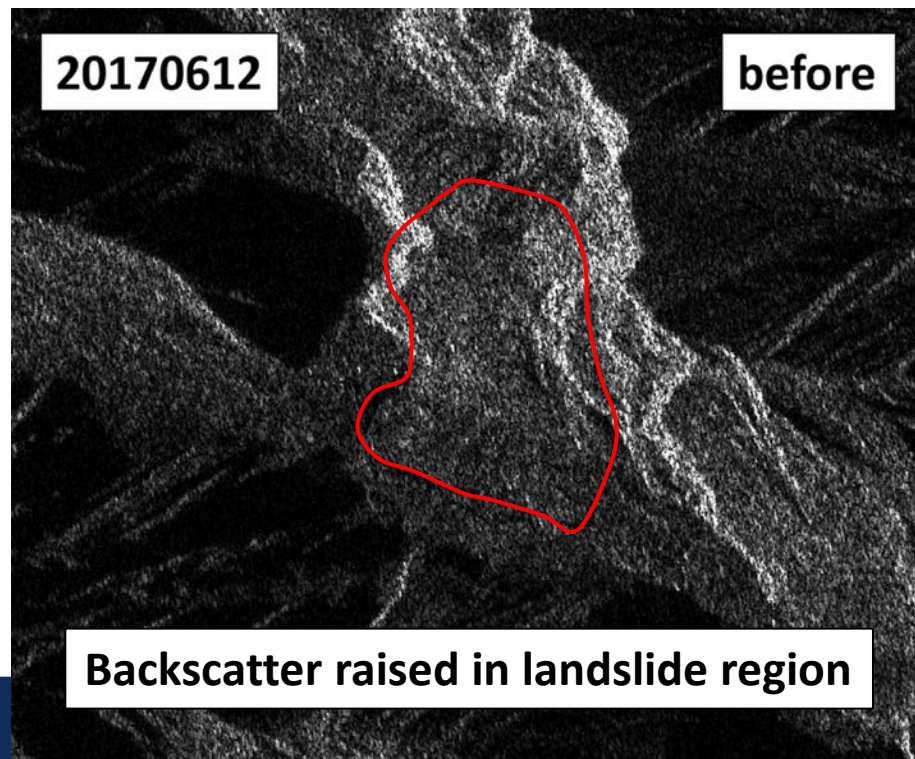
2017年6月26-30日, 丹麦 哥本哈根

D-InSAR results for Sentinel-1 data

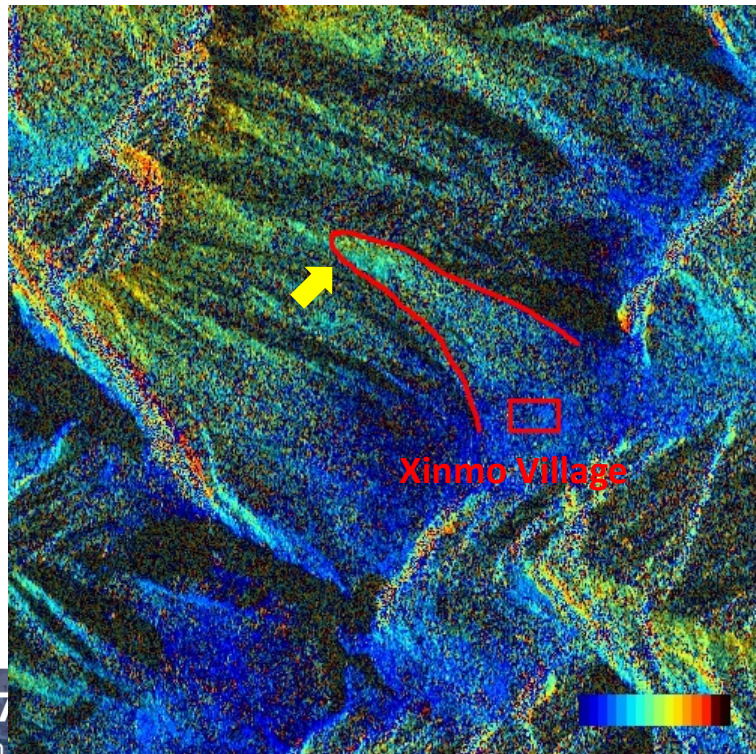
Google Earth™ image



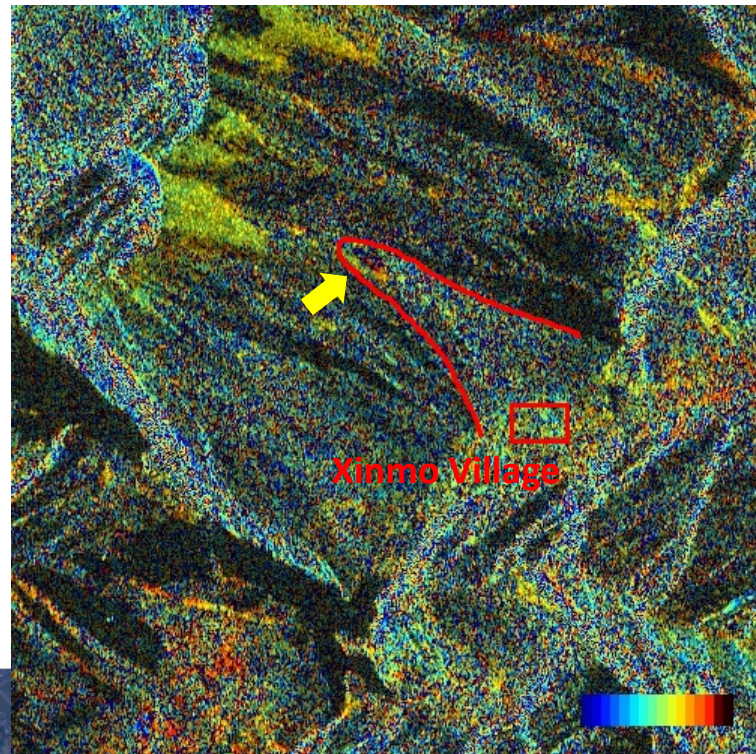
Amplitude change



20170315-20170327



20170607-20170619



Summary for monitoring landslides

- DSI can detect wide-area landslides and monitor local-scale landslides with high precision.
- More points are detected by DSI than PSI and SBAS.
- DSI and L-band SAR data are more suitable for landslide monitoring in vegetated terrains.

Conclusion

- High-resolution stereoSAR was used to improve the quality of InSAR DEM in vegetated hilly areas.
- HR&MR SAR data stacks were applied for monitoring urban subsidence and infrastructures. The results from Sentinel-1 data were effective for observing the bridge deformation.
- DS-InSAR was used with PS-InSAR for monitoring landslide stability. The preliminary InSAR results are promising in steep & vegetated mountainous areas.

